Title: Energetic demands of extreme temperatures reduce cryptobenthic coral reef fish diversity and functioning

Authors: Simon J. Brandl[1,2,3,4]*†, Jacob L. Johansen[5,6]†, Jordan M. Casey[3,4], Luke Tornabene[7], Renato A. Morais[8,9], John A. Burt[6]

† indicates shared first authorship

***Corresponding author:** Simon J. Brandl, simonjbrandl@gmail.com,

(ORCID: 0000-0002-6649-2496)

Affiliations:

[1] Department of Biological Sciences, Simon Fraser University, Burnaby, BC, Canada

[2] CESAB - FRB, 5 Rue de l'École de Médecine, 34000, Montpellier, France

[3] PSL Université Paris: CNRS-EPHE-UPVD USR3278 CRIOBE, Université de Perpignan, Perpignan, France

[4] Laboratoire d'Excellence "CORAIL," Perpignan, France

[5] Hawai'i Institute of Marine Biology, University of Hawai'i at Manoa, Kane'ohe, HI, USA

[6] Marine Biology Laboratory, Centre for Genomics and Systems Biology, New York University Abu Dhabi, Abu Dhabi, United Arab Emirates

[7] School of Aquatic and Fishery Sciences and the Burke Museum of Natural History and Culture, University of Washington, Seattle, WA, USA

[8] ARC Centre of Excellence for Coral Reef Studies, James Cook University, Townsville, QLD, Australia

[9] College of Science and Engineering, James Cook University, Townsville, QLD, Australia

Abstract:

Environmentally mediated transformations of ecological communities can influence ecosystem functioning. Coral reef fishes are hypothesized to be vulnerable to globally rising temperatures, but cascading effects of organismal tolerances on the assembly and functioning of reef fish communities are largely unknown. Here, we show that cryptobenthic reef fish assemblages on the world's hottest reefs in the southern Arabian Gulf have half the species density and less than 25% the individual density compared to the thermally benign nearby Gulf of Oman, despite equal availability of live coral substrate. This pattern is not driven by intrinsic organismal temperature tolerances. Rather, the impoverished body condition of populations in the Arabian Gulf emphasizes the increased energetic costs of growth and homeostasis at higher temperatures, while intraspecific dietary differences between locations suggest that Arabian Gulf populations need to meet these energetic costs with a different and narrower set of prey resources. By creating an energetic double jeopardy, these conditions prohibit the persistence of small-bodied species with high mass-specific metabolisms and, ultimately, cause the reduced production, transfer, and replenishment of biomass through cryptobenthic fish assemblages. Consequently, future reefs may lose a critical building block of their fast-paced dynamics, independent of live coral loss.

Introduction:

Why do some species occur in a given location while similar taxa are missing? And how do resulting species assemblages affect rates of ecological processes? As escalating human impacts on the biosphere deplete and re-shuffle biological communities across

ecosystems[1,2], answers to these questions are key to our quest to preserve biodiversity and ecosystem services to humanity[3,4].

A species' presence at a given location is mediated by a hierarchical interplay between organismal traits (e.g., temperature tolerance, trophic niche), environmental conditions (e.g., temperature, salinity), biogeographic history, and stochastic events (e.g., extinction, dispersal, lottery dynamics)[5–8]. Furthermore, the identity and diversity of species affect rates of ecosystem functioning, including processes that are critical to human well-being, such as primary or consumer productivity[9–11]. However, by modifying abiotic conditions, species' niches, and biotic interactions, global stressors such as climate change can interfere with these dynamics through numerous pathways[12–14]. At the organismal level, changes in environmental factors, particularly temperature, affect internal physiological processes[15], which, if not lethal, will alter organismal energy expenditure[16–18]. Changes in organismal energy budgets subsequently drive resource acquisition (e.g. feeding rates, prey species) and how resulting energy is allocated to life-supporting processes (homeostasis), growth, and reproduction[19–22]. Dynamics of energy acquisition and investment, which are often investigated through the lens of ecological niche and fitness, are the basis of modern coexistence theory and critical for our understanding of community assembly dynamics[23] and the rate of ecological processes that underpin energy and nutrient fluxes through ecosystems[24]. Integration across levels of biological organization is, therefore, crucial to understand the effects of global environmental change on our planet's ecosystems[25].

Coral reefs are the most diverse marine ecosystem, and their productivity provides vital services for more than 500 million people worldwide[26]. Scleractinian

corals, the foundation species of tropical reefs, show high thermal sensitivity that has led to the rapid global decline of coral reef ecosystems[27]. In wake of losing coral habitat, communities of the most prominent reef consumers, teleost fishes, can decline or shift in composition[28–31], which directly affects the provision of resources to people dependent on reef fisheries[32]. Nevertheless, recent evidence suggests that many fish species will be able to cope with (or even benefit from) live coral loss, at least in the short-term[32–34]. However, tropical marine ectotherms are typically adapted to a relatively narrow thermal environment, so reef fishes may also be vulnerable to the direct effects of changing water temperatures[16,35,36]. Consequently, the direct responses of reef fishes to climate change and their potential to adapt to different thermal regimes might be as important as indirect, habitat-mediated responses[37–39].

Despite marked differences in species-specific tolerances to higher temperatures[40–44], most reef fish species suffer from non-lethal[45] adverse physiological, developmental, or behavioral responses when exposed to temperatures outside of their normal range. Current understanding suggests long-term deleterious effects on reef fish populations in the wild[37], but few cases of direct temperature-mediated population declines have been documented for *in situ* reef fish communities[46]. One factor that ameliorates the adverse effects of rising temperatures in the wild may be transgenerational acclimation and adaptation, which can enhance the performance of offspring in higher temperatures through developmental, genetic, or epigenetic pathways[39,47]. Transgenerational adaptation has been shown in a few model species[39,47,48], but demands increased energetic investments[47,49]. It is presently unresolved whether this process can truly enhance the survival of reef fishes in

competitive, uncontrolled environments and how species-specific temperature tolerance differences may mediate coexistence in ecological communities.

Cryptobenthic fishes are the smallest of all reef fishes, rarely exceeding 50mm in maximum body size[50]. They account for almost half of all reef fish species and are numerically abundant and ubiquitous on reefs worldwide[50–53]. Due to their small body size, these fishes have evolved a unique life history strategy of rapid growth, high mortality, and continuous larval replenishment, and they may play an important role in coral reef trophodynamics[54]. Their small body size and associated life-history also promise exceptional traceability concerning the effects of, and responses to, increasing temperatures[50]. Limited gill surface area, unfavorable mass to surface ratios, high mass-specific metabolism, and other physiological challenges resulting from their minute size suggest that cryptobenthics are particularly susceptible to temperature fluctuations[42,50,55]. Due to their limited mobility and close association with the benthos[56], mitigation of temperature extremes through migration is often not viable, and notable community composition shifts following changes in the benthic community structure have been detected[31,57]. However, their extremely high generational turnover (7.4 generations per year in some species[54,58]) and prevalence of benthic clutch spawning and parental care[50] may make them ideally suited for transgenerational adaptation to changing conditions[37]. In fact, an extremely fast evolutionary clock has been implicated as a driver for rapid speciation in cryptobenthic fishes[59], which may permit similarly fast microevolutionary changes (i.e., rapid adaption). Thus, cryptobenthic fishes may be well-suited to detect the impact of environmental change on organisms and populations,

with promising insights into whether transgenerational plasticity or adaptation can provide pathways to the persistence of coral reef fishes in warming oceans.

Here, we quantify cryptobenthic community structure, species- and population-specific physiological and dietary traits, and contributions to ecosystem functioning in the world's hottest coral reef environment, the southeastern Arabian Gulf, and we compare the resulting patterns with the spatially proximate, but more environmentally benign, Gulf of Oman. Specifically, the goal of our study was to 1) describe cryptobenthic fish assemblages across the two locations, 2) identify organismal traits that permit or preclude existence in the Arabian Gulf, and 3) determine the consequences of these results for the production, provision, and renewal of cryptobenthic fish biomass[25].

Results:

Reefs in the shallow southern Arabian Gulf can range from 16º C in the winter months to over 36º C in the summer, while reefs in the nearby Gulf of Oman fluctuate within a much narrower temperature range (approximately 22º C to 32º C)[60]. Maximum temperatures on reefs along the Arabian Gulf coast of the United Arab Emirates mirror forecasted temperatures for most tropical coral reefs in the end of the century[61]. Despite the seemingly unfavorable conditions for tropical reef building corals, corals have persisted in this region for approximately 15,000 years, with the modern coastline harboring coral reef structures for circa 6,000 years[61]. Therefore, the Arabian Gulf represents an exceptional natural laboratory to examine the capacity of reef organisms

to cope with unfavorable conditions and how this influences the diversity and dynamics that underpin modern coral reefs (Fig. 1a,b).

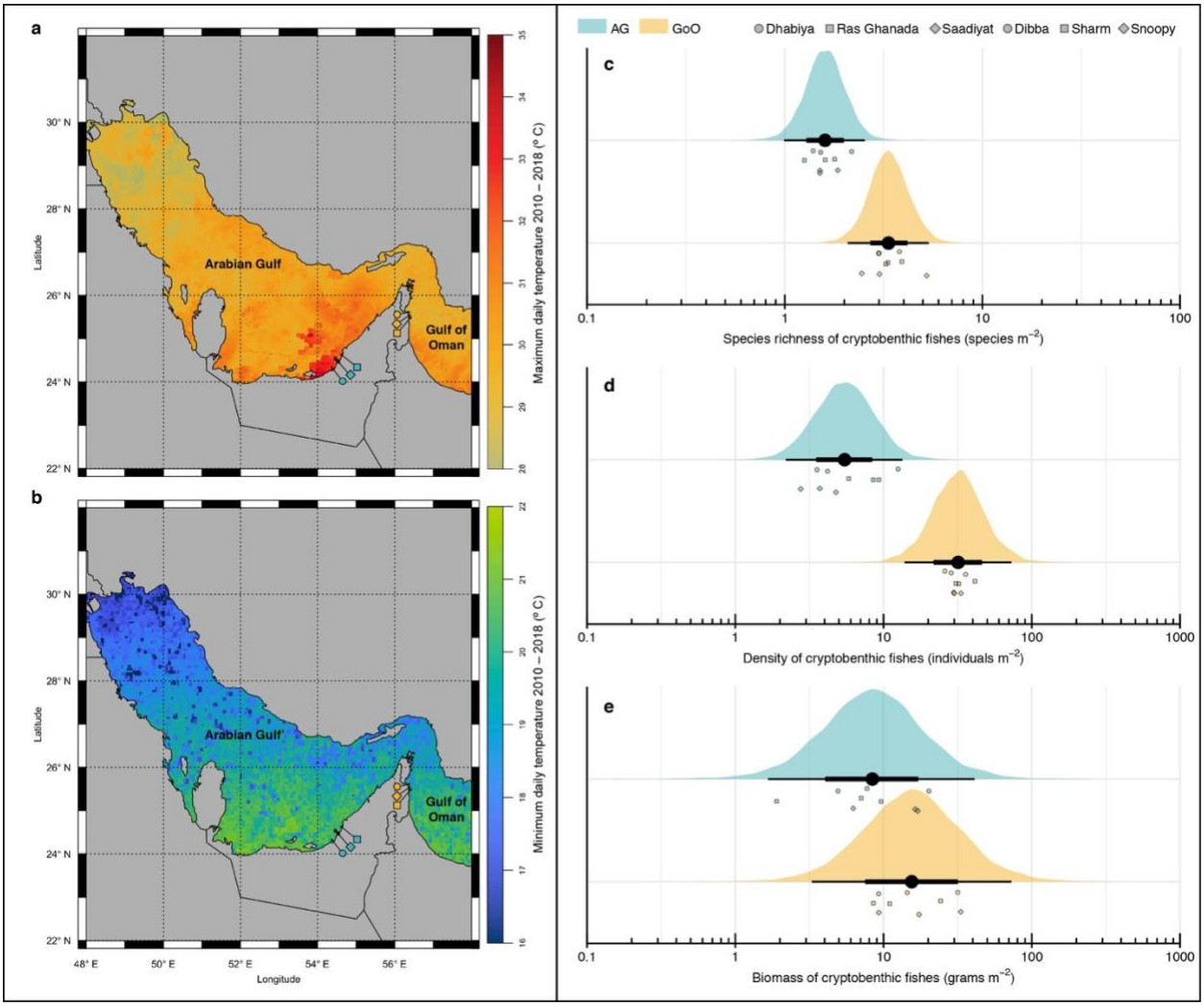

Fig. 1 | Map of the study system and community structure of cryptobenthic reef fish communities in the Arabian Gulf (AG) and Gulf of Oman (GoO). (**a–b**) Maximum and minimum daily temperature estimates for the AG and GoO between 2010 and 2018 (obtained from MODIS Aqua; https://oceandata.sci.gsfc.nasa.gov/MODIS-Aqua/Mapped/Daily/4km/sst), with the study sites indicated. (**c**) Species density and (**d**) individual density of cryptobenthic reef fishes was markedly higher on reefs in the GoO, while (**e**) biomass did not substantially differ between the two locations. Density curves represent predicted values based on 1,000 draws from Bayesian hierarchical linear models testing for differences between locations, while black caterpillar plots represent their means, 50%, and 95% credible intervals. Circles, squares, and diamonds represent raw values from the respective sites in each location, jittered on the y-axis.

Cryptobenthic reef fish assemblages markedly differed between the Arabian Gulf and the Gulf of Oman. Reefs in the Gulf of Oman harbored a higher diversity (Bayesian

hierarchical model estimate: *Gulf of Oman:* β = 0.73 [0.44, 1.01; lower and upper 95% credible interval]) and density (*Gulf of Oman:* β = 1.77 [1.03, 2.58]) of cryptobenthic fishes (Fig. 1a,b), but standing biomass estimates were comparable (*Gulf of Oman:* β = 0.63 [-0.54, 1.71]; Fig. 1c). Similarly, the composition of cryptobenthic communities greatly varied between the two locations (Fig. 2a), with no overlap among convex hull polygons in the non-metric multidimensional scaling (nMDS) ordination and a strong effect of *Location* in the PERMANOVA using a site-by-species dissimilarity matrix (*Location*: *df* = 1, *F* = 13.58, *P* = 0.001, *R2* = 0.46). There were 29 unique species in the Gulf of Oman, 13 unique species in the Arabian Gulf, and 16 species shared among the two locations. Importantly, of the 29 unique Gulf of Oman species, 89.7% have records from the northern Arabian Gulf in Kuwait and Saudi Arabia (but not the southeastern region), where summer conditions are much less extreme[62] (Fig 1; Table S1). In contrast to the cryptobenthic fish community, there were no differences in coral cover (Bayesian hierarchical model: *Gulf of Oman:* β = 0.02 [-1.30, 1.42]) nor overall benthic community structure as revealed by a PERMANOVA (*Location*: *df* = 1, *F* = 1.63, *P* = 0.187, *R2* = 0.09; Fig. 2b). Thus, despite broadly comparable benthic conditions, including similar live coral cover, cryptobenthic fish assemblages strongly differed between the two locations.

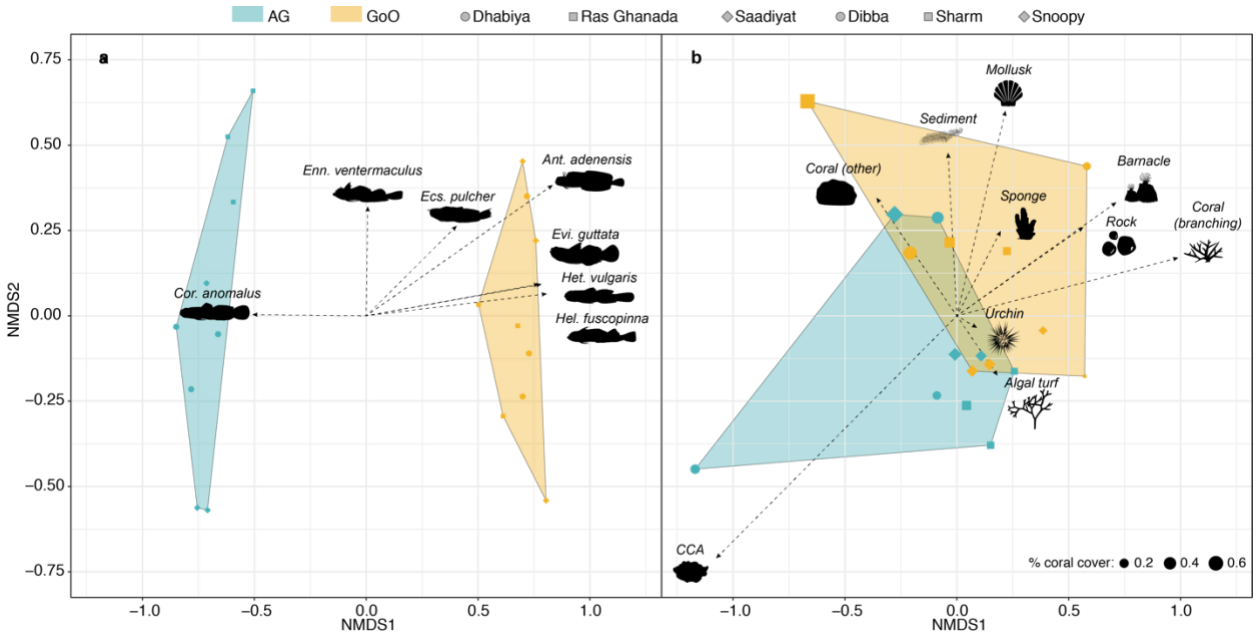

Fig. 2 | Community composition of cryptobenthic reef fishes and benthic functional/taxonomic groups in the Arabian Gulf (AG) and Gulf of Oman (GoO). (**a**) Biplot of a non-metric multidimensional scaling (nMDS) ordination on cryptobenthic fish communities, with the arrows indicating the position and strength of the seven most important species. (**b**) Biplot of an nMDS on benthic functional groups, with the influence of all groups indicated with arrows. Convex hull polygons delineate the two locations. Each point represents a sample station at a particular site, with the shape size in (**b**) scaled by percent live coral cover.

We then tested whether organismal temperature tolerance can explain the absence of species from the thermally extreme southeastern Arabian Gulf, despite their recorded presence in more benign parts of the Arabian Gulf. Notwithstanding distinct thermal regimes at the two locations and the drastic differences in cryptobenthic fish assemblages, species-specific critical thermal tolerance limits did not explain the absence of three common Gulf of Oman species in the Arabian Gulf (Fig. 3). The mean critical thermal maximum tolerance limits (ct_{max}) of all species, regardless of origin, equaled or surpassed the maximum summer temperatures typically recorded in the Arabian Gulf (36.0 ºC). *Helcogramma fuscopinna* (a Gulf of Oman species) had the lowest heat tolerance at 36.0 ± 0.11 ºC, while *Coryogalops anomolus* from the Arabian

193 Gulf had the greatest heat tolerance (38.4 ± 0.06 ºC). While there were no population
194 differences in heat tolerance for *Enneapterygius ventermaculus* (possibly due to limited
195 samples from the Gulf of Oman), the Arabian Gulf population of *Ecsenius pulcher*
196 showed considerably greater heat tolerance than their Gulf of Oman counterparts,
197 providing evidence for enhanced thermal tolerance in this species. Despite considerable
198 interspecific differences and evidence for intraspecific thermal plasticity (Table S2),
199 mean predicted maximum posterior heat tolerances of all species restricted to the Gulf
200 of Oman were within the 95% bounds of the species present in the Arabian Gulf.
201 In terms of critical thermal minima (ct_{min}), all species, regardless of origin,
202 tolerated the minimum winter temperature of the UAE Arabian Gulf at 16 ºC. Among
203 individuals sampled from the Gulf of Oman population, *E. pulcher* had the greatest
204 tolerance to cold (ct_{min} = 11.3 ± 0.1 ºC), while *E. ventermaculus* had the poorest
205 tolerance (13.3 ± 0.1 ºC). The cold-tolerance of *E. ventermaculus* in the Arabian Gulf
206 substantially exceeded its Gulf of Oman counterpart (Table S3), which provides
207 evidence from a second population for intraspecific plasticity in thermal tolerances
208 across the two locations. Although there were again species-specific differences in the
209 critical thermal minimum, mean cold tolerances of all Gulf of Oman species also fell
210 within the 95% credible bounds of the species present in the Arabian Gulf (Fig. 3a).
211

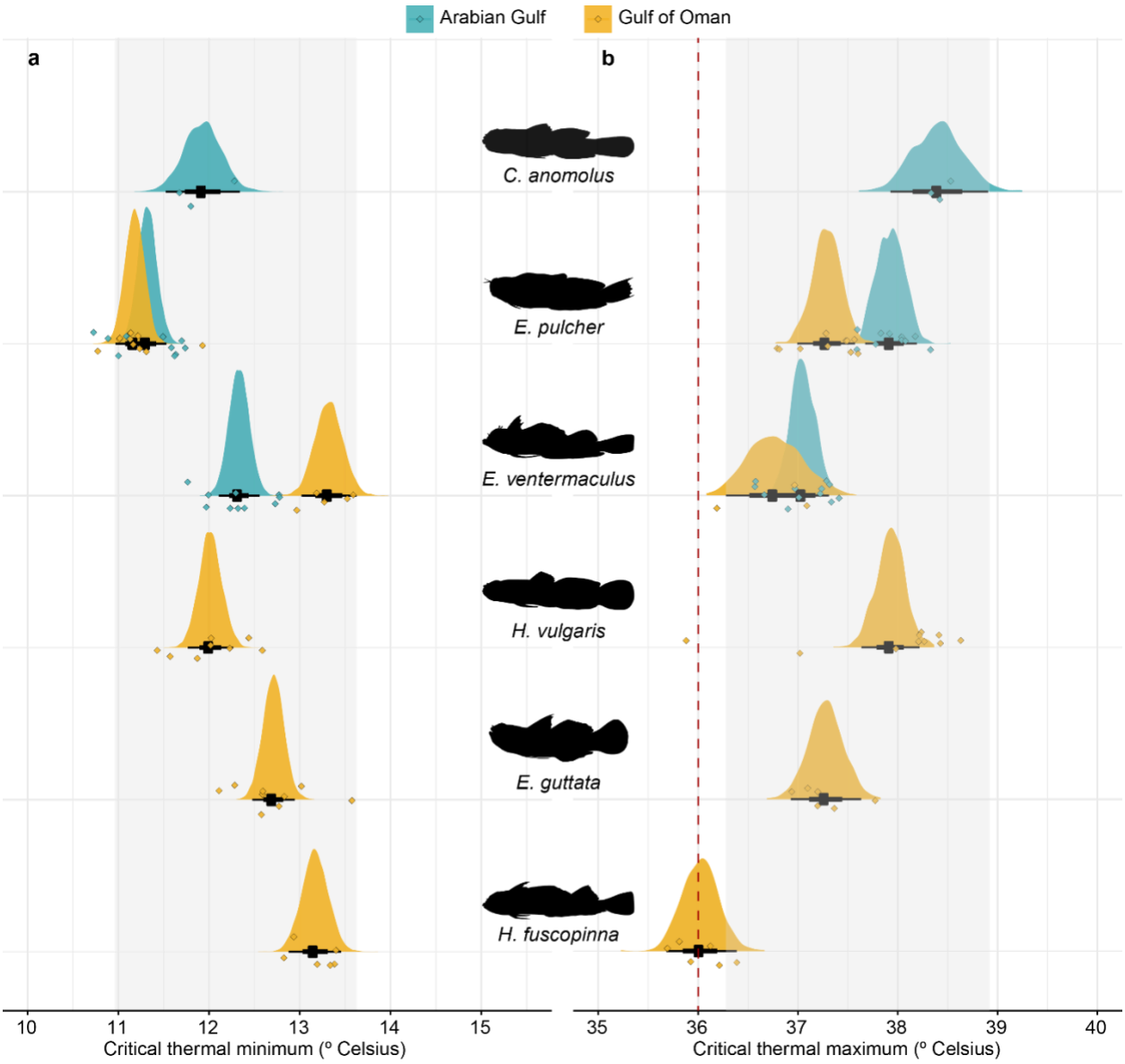

Fig. 3 | Critical thermal tolerance limits of cryptobenthic fish species from the Arabian Gulf and Gulf of Oman. (**a**) Critical thermal minima ranged between 11.9 ºC and 13.3 ºC, well below the minimum recorded winter temperature for the southern Arabian Gulf (16.0 ºC). (**b**) Critical thermal maxima ranged between 36.0 ºC and 38.4 ºC, but they were above or equal to the maximum recorded summer temperature in the Arabian Gulf (36.0 ºC; red dashed line). Density curves represent fitted values based on 10,000 draws from Bayesian linear models that test for differences among all populations, while black caterpillar plots represent their means, 50%, and 95% credible intervals. Diamonds represent raw values, jittered on the y-axis. Grey boxes delineate the range of the 95% credible intervals obtained for the three species present in the Arabian Gulf.

To further examine potential drivers of cryptobenthic community structure, we quantified species' diets in the two locations using gut content DNA metabarcoding[63]

across 88 individuals belonging to six species (*C. anomolus*, *E. pulcher*, and *E. ventermaculus* [Arabian Gulf and Gulf of Oman populations]; *Antennablennius adenensis*, *Eviota guttata*, and *Hetereleotris vulgaris* [Gulf of Oman only]). We targeted the cytochrome *c* oxidase subunit I (COI) gene region with primers that preferentially amplify metazoans and the 23S rRNA gene region with primers designed to amplify algae. Across all examined fishes, COI metabarcoding yielded a total of 547 unique operational taxonomic units (OTUs), while 23S metabarcoding yielded 3,009 unique exact sequence variants (ESVs). Bipartite dietary network trees and modularity analyses for the COI marker showed strong separations between the Arabian Gulf and Gulf of Oman populations (Fig. 4). The COI network contained five distinct modules (modularity = 0.472), with 92.3% of individuals from the Arabian Gulf distributed across two modules. Module V contained seven out of ten individuals of *C. anomolus* from the Arabian Gulf, 8 out of 9 individuals of *E. ventermaculus* from the Arabian Gulf, and one *E. guttata* from the Gulf of Oman. The remaining individuals of *C. anomolus* and *E. ventermaculus* from the Arabian Gulf clustered with *E. pulcher* from the Arabian Gulf (five out of seven), four Gulf of Oman individuals of *C. anomolus*, and a single *H. vulgaris* in module II (Fig. 4a,b). The 23S marker also revealed five modules (modularity = 0.359) but showed an even stronger regional separation. All individuals from the Arabian Gulf (except for one *C. anomolus*) were united in a single module (module III), which contained no Gulf of Oman individuals (Fig. 4c,d). While some species separated into distinct modules, location specific differences superseded taxonomic boundaries. With the exception of *C. anomolus*, species occurring in both locations showed strong dietary differences, while broadly overlapping with other species in the Gulf of Oman.

Prey diversity rarefaction curves in the Gulf of Oman showed that *E. pulcher*, a purportedly herbivorous species[64], ingested the widest variety of animal prey species (COI marker), followed by *E. ventermaculus* (Fig. S1). For both species, Gulf of Oman populations consumed a higher diversity of prey items than Arabian Gulf populations. Only *C. anomolus* showed no clear difference in extrapolated values (although diversity was higher for Gulf of Oman populations for the interpolated value). For algal prey items (23S marker), prey diversity was again higher in Gulf of Oman populations of *E. pulcher* and *E. ventermaculus*, while the opposite was evident for *C. anomolus*. Overall, Gulf of Oman populations of *E. ventermaculus* ingested the highest autotroph prey diversity, followed by Arabian Gulf populations of *C. anomolus*.

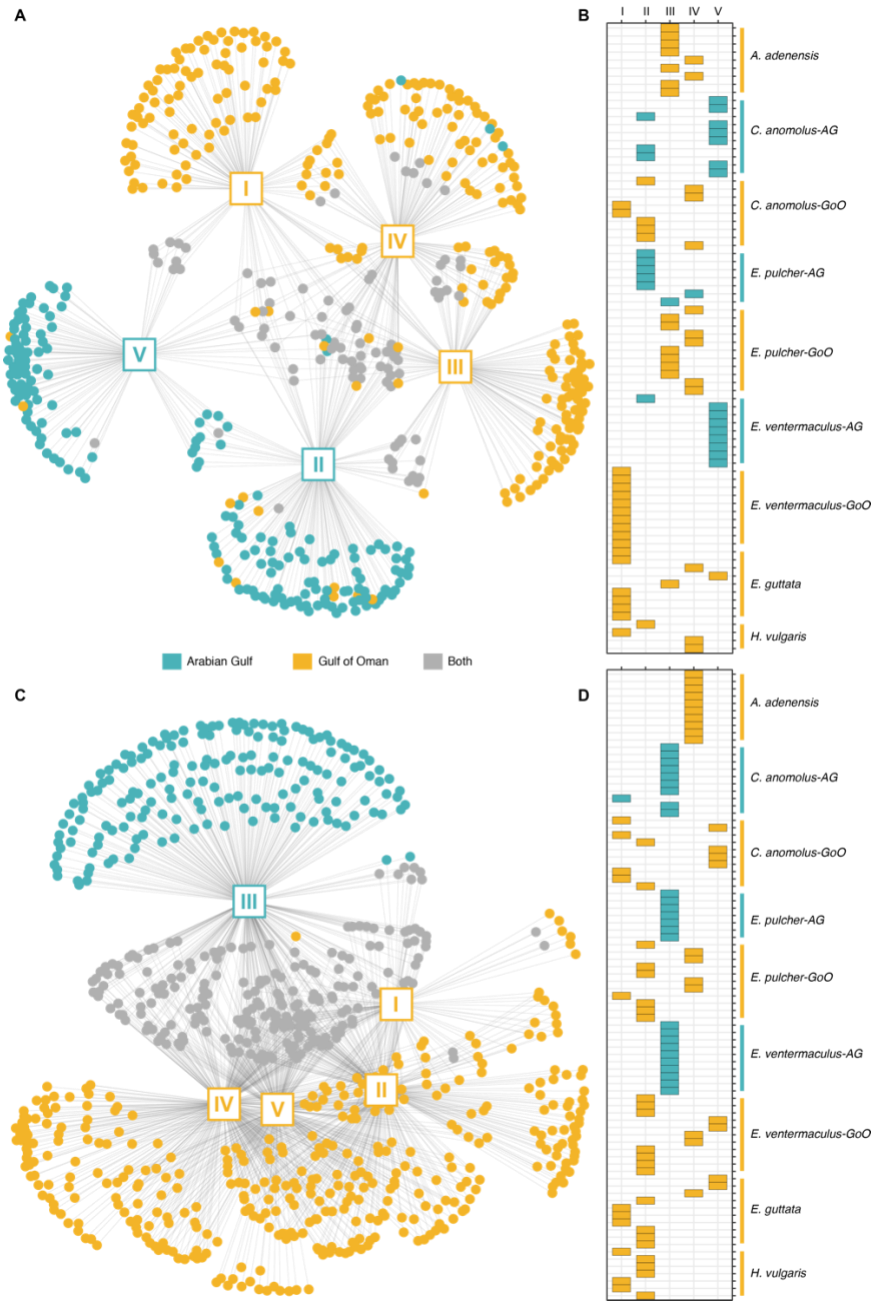

Figure 4 | Diet network trees and modularity mosaics showing differences in ingested prey items and individual-based module membership for COI (a,b) and 23S (c,d) markers. (a,c) Squares with roman numerals represent the recovered modules as nodes in the network tree, while dots represent unique prey items. Blue dots are OTUs (COI) or ESVs (23S) found only in individuals from the Arabian Gulf, gold symbols are from the Gulf of Oman individuals, and grey symbols represent prey items found in individuals from both locations. **(b,d)** Results of the modularity analysis with modules (I-V) as columns and individuals within each species as rows. Colored squares indicate membership in a given module.

We further examined the potential organismal and ecosystem-wide energetic consequences of thermal regimes and resource availability between the two locations by first assessing length-weight relationships of three co-occurring species, and then by modeling individual-based growth and mortality to estimate community-wide biomass cycling. We employed Bayesian linear models to test the effects of total length (*TL*) and *Location* on *Weight*, which showed clear effects of *Location* across all species, with Gulf of Oman populations consistently having higher weights for a given body length (*E. ventermaculus*: *Gulf of Oman:* β = 0.16 [0.13, 0.19], *C. anomolus*: *Gulf of Oman:* β = 0.15 [0.09, 0.21], and *E. pulcher*: *Gulf of Oman:* β = 0.19 [0.14, 0.25]) (Fig. 5). Notably, empirical values for the largest individuals of *C. anomolus* from the Arabian Gulf were consistently below the model fit, suggesting worse body conditions than predicted by the model and substantially worse body conditions than Gulf of Oman individuals of comparable size (Fig 5b). In contrast, no clear differences emerged between the abundances of the three species' populations across locations (effect size uncertainties intersected zero), although *E. ventermaculus* (*Gulf of Oman:* β = 0.89 [-1.08, 2.86) and *E. pulcher* (*Gulf of Oman:* β = 3.46 [-0.42, 9.93]) showed a trend toward lower abundances in the Arabian Gulf, while *C. anomolus* exhibited the opposite trend (*Gulf of Oman:* β = -0.94 [-3.82, 1.69]).

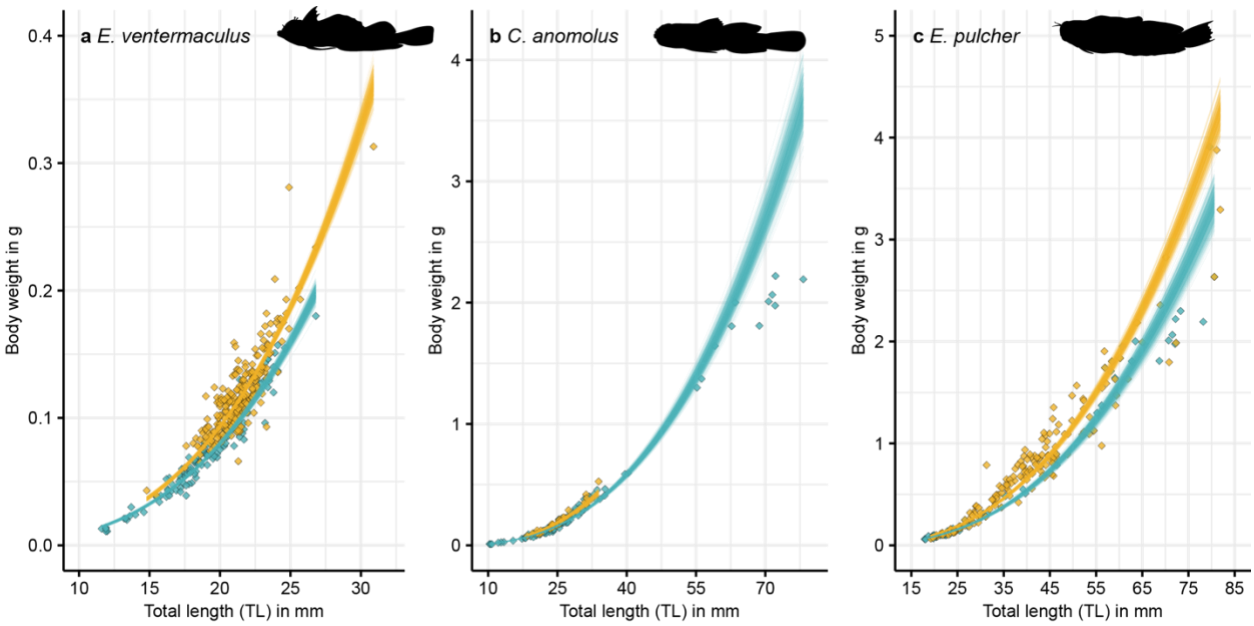

Figure 5 | Relationships between total length (TL) and body weight in populations of *Enneapterygius ventermaculus* (a), *Coryogalops anomolus* (b), and *Ecsenius pulcher* (c) in the Arabian Gulf (blue) and Gulf of Oman (gold). Each line represents a fitted draw from 500 iterations based on the posterior parameters from a Bayesian model regressing length against weight (thus showing model fit uncertainty). Diamonds represent raw values for individual fishes.

Finally, modeling individual-based growth and mortality for cryptobenthic fish communities at each site revealed strong differences in the ecological dynamics that underpin ecosystem functioning between the Arabian Gulf and Gulf of Oman (Fig. 6). Biomass production was almost one order of magnitude higher on reefs in the Gulf of Oman (0.231 ± 0.025 [mean ± SE] g d^{-1} m^{-2}) compared to the Arabian Gulf (0.038 ± 0.014 g d^{-1} m^{-2}), while consumed biomass was more than five times higher (0.039 ± 0.015 vs. 0.007 ± 0.001 g d^{-1} m^{-2}). Turnover was also higher in the Gulf of Oman (0.017 ± 0.005 % d^{-1}) compared to the Arabian Gulf (0.006 ± 0.005 % d^{-1}). Therefore, reefs in the two locations exhibit contrasting productivity dynamics at various levels of organization. In the Arabian Gulf, individual fishes accumulate less body mass per

millimeter of body length and collectively, cryptobenthic communities produce, provide, and replenish consumer biomass at much lower rates than Gulf of Oman communities.

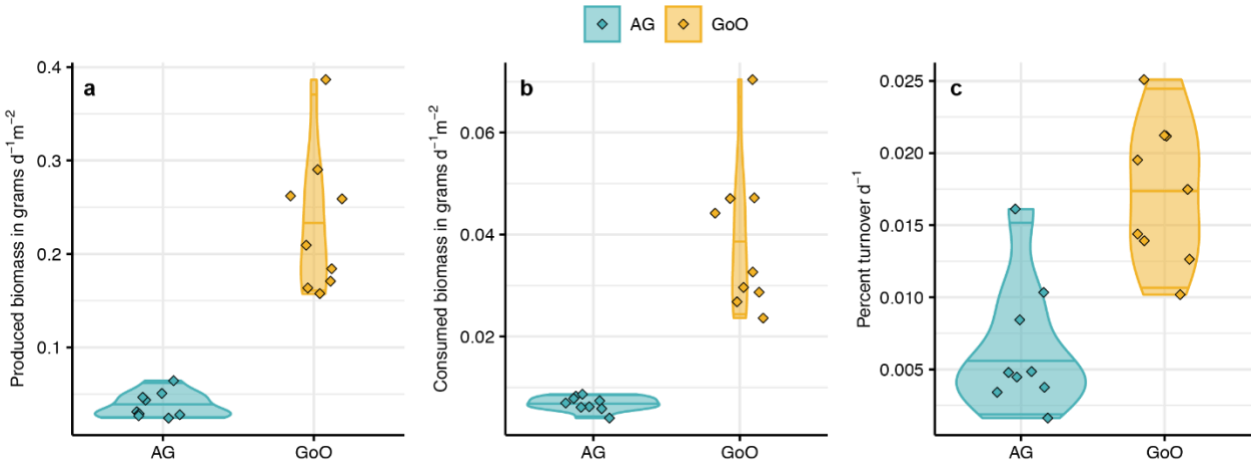

Figure 6 | Model estimated biomass production, consumption, and turnover in cryptobenthic fish assemblages across the two locations. (**a**) Produced biomass (grams of fish tissue grown per day and m_2). (**b**) Consumed biomass (grams of fish tissue perished per day and m_2). (**c**) Percent turnover (renewal of produced and consumed biomass per day). Violin plots and lines represent medians and variance estimates (95% quartiles) for the three metrics across the two locations. Diamonds represent values for each sampled cryptobenthic reef fish community across the six sites (three per site).

Discussion:

As rapid environmental change sweeps across the Earth's ecosystems, garnering an understanding of the processes that underpin local community structure and ecosystem functioning is urgent. Here, we show that cryptobenthic fishes on reefs exposed to the world's most extreme temperature regime in the southeastern Arabian Gulf have reduced diversity, abundance, and body condition compared to reefs with more moderate temperatures in the nearby Gulf of Oman, despite similarities in live coral cover and benthic community structure. While species with populations in both locations exhibit thermal plasticities that enable survival in Arabian Gulf conditions, species-

specific temperature tolerances are not the main driver of species presence/absence in the Arabian Gulf. Rather, poor body condition in Arabian Gulf populations suggest that physiological responses to the Arabian Gulf conditions might invoke energetic costs that can only be borne by species with low metabolic demands. Furthermore, intraspecific dietary differences indicate that cryptobenthic fishes in the Arabian Gulf need to meet these increased costs with a distinct and restricted suite of prey items. These individual energetic challenges have far reaching consequences for ecosystem-scale energy and nutrient fluxes; even conservative estimates of cryptobenthic reef fish productivity in the Arabian Gulf are an order of magnitude lower than the Gulf of Oman. Our results indicate that cryptobenthic reef fish assemblages on future coral reefs may be shaped by species-specific individual energy deficits that decrease the rate of biomass production, transfer, and renewal through small vertebrate consumers, thereby eroding a cardinal component of heterotrophic coral reef productivity[54].

Organismal responses

As the smallest and shortest-lived marine vertebrates, responses of cryptobenthic fishes to extreme temperatures should be easy to trace[50]. Yet, critical thermal tolerances of all tested species from both locations were equal to or greater than the extreme maximum summer temperatures of the southeastern Arabian Gulf[43,45,65]. The high intrinsic tolerance of species from the relatively cool Gulf of Oman aligns with previous results of high, short-term critical thermal tolerances in cryptobenthics[43]. Furthermore, swift generational turnover in cryptobenthic fishes could facilitate transgenerational thermal plasticity and increased thermal tolerance[54,58]. Collectively, this should have permitted

their colonization and persistence in the geologically young southeastern Arabian Gulf[66], since no hard biogeographic boundary exists between the Gulf of Oman in the Arabian Gulf[60]. Indeed, 26 out of 29 (89.7%) cryptobenthic fish species from the Gulf of Oman that were absent from the southeastern Arabian Gulf have been recorded in the cooler Arabian Gulf regions of Saudi Arabia and Kuwait (Table S1)[62,67,68]. Thus, neither thermal tolerances to short-term temperature extremes nor biogeographic history are likely to drive the observed depauperate cryptobenthic communities on Earth's hottest coral reefs.

Instead, temperature-driven demands on an individual's energetic budget and the inability of small-bodied fishes to meet these demands appear to mediate existence on these extreme reefs. Transgenerational acclimation or adaptation of fishes to increasing temperatures can come with substantial energetic costs[39,47,69] that are reflected in reduced body condition[22,70,71]. These costs are evident in the lower mass per unit body length of Arabian Gulf populations in the three examined species. Although shifts in transgenerational temperature tolerance may permit survival and adequate performance in controlled laboratory conditions[39,47], our results show that acclimation to warmer water and its associated energetic costs may not be viable for most cryptobenthics in natural environments where they continuously engage in costly activities such as foraging and escaping predators[70].

In the southeastern Arabian Gulf, this energetic dilemma may be further exacerbated by fundamentally different dietary resources and reduced prey diversity; indeed, gut content metabarcoding revealed a different and narrower range of both primary and secondary prey resources ingested by individuals from the Arabian Gulf.

Shifts in dietary composition can require changes in digestive morphology and processes that further alter species' energy budgets[72,73], while a lower diversity of prey items can reduce individual and population persistence[74,75]. Naturally, energetic challenges would be even greater if prey in the Arabian Gulf has less favorable nutritional profiles or energy densities[76]. While we did not investigate differences in diet quality (i.e., nutrient content) across locations, large reef fish species in the Arabian Gulf have been shown to ingest unusual diets dominated by nutritiously poor benthic invertebrates[77].

Moreover, the goby *Coryogalops anomolus* was the only cryptobenthic species to show weakly distinct prey composition between locations and higher autotroph prey richness in the Arabian Gulf, and it was also the only species with a higher abundance and larger body size in the Arabian Gulf as compared to the Gulf of Oman. This species also had a less pronounced reduction in body condition from the Gulf of Oman to the Arabian Gulf compared to *E. pulcher* and *E. ventermaculus*. As opposed to most dominant cryptobenthic genera in the Arabian Gulf and Gulf of Oman (e.g. *Ecsenius, Eviota, Enneapterygius*, etc.), the goby genus *Coryogalops* belongs to a clade that contains many non-reef associated species from comparatively extreme habitats[78,79] For example, *Coryogalops* often inhabit tidepools and other shallow environments exposed to fluctuating temperatures and salinity where they rely on a sedentary lifestyle with low energetic costs[80,81]. Thus, the persistence of *C. anomolus* in the southeastern Arabian Gulf may reflect an adaptation to extreme environments afforded by its evolutionary history of belonging to a lineage of non-reef, extreme habitat specialists.

Our results indicate that species-specific capacities to cope with the energetic costs of inhabiting extreme environments, rather than the direct effects of temperature *per se* or its effect on benthic community structure (cf.[65]), underpin the reduced diversity and abundance of cryptobenthic fishes on these extreme reefs. For cryptobenthics, which already exhibit high energetic demands per gram of body mass and rapid growth[50], increased cost of growth and homeostasis appear to represent a significant challenge. Along with environmentally-driven differences in prey composition and diversity (as well as potential reductions in nutritional value or energetic densities), this may create an energetic double jeopardy that represents an insurmountable obstacle for many cryptobenthic species. Further decreases in body size (a universal physiological response to warmer temperatures[18,22]) might simply not be possible for many cryptobenthic reef fishes that are already at or near the physical minimum body size for vertebrates[50,55,82]. Therefore, our findings provide novel evidence for the consequences of climate change on organismal performance[83,84], including their ramifications for species persistence and community assembly[85], from highly-vulnerable, tropical ectotherms in a natural setting.

Ecosystem-scale consequences

The individual-based energetic challenges that appear to govern community assembly in the southeastern Arabian Gulf create a sobering perspective on coral reef ecosystem functioning in a warming ocean. Coral reefs are some of the most productive marine ecosystems[86] that are sustained through a variety of energetic pathways[87–90]. Among these pathways, benthic productivity[91] and its assimilation and transfer through

cryptobenthic reef fishes represents an important bottom-up flux of energy and nutrients to higher trophic levels[54]. The dramatic differences in biomass production, transfer, and turnover between cryptobenthic fish communities in the Arabian Gulf and Gulf of Oman suggest that the role of cryptobenthics as vectors of energy and nutrients to larger consumers may be stymied in hot waters. In fact, yearly productivity estimates for cryptobenthic fishes in the Arabian Gulf may be even lower than our model suggests due to the decreased individual-level production of body mass per unit body size and the influence of seasonality effects on growth. Both winter and summer temperatures in the southeastern Arabian Gulf are unfavorable for growth and effectively interrupt the growing season of cryptobenthic fishes (which are predominantly annual species), much as they do with fishes from other seasonal ecosystems[92]. Yet, neither environmental limits on the growing season, nor decreased individual mass per unit body size were considered in the model, which held temperature constant at the mean annual temperature to allow constant growth throughout the year and used constant length-weight coefficients for both locations. Inclusion of these factors would almost certainly further reduce productivity estimates for the Arabian Gulf reefs.

The Gulf of Oman reefs included in this study may be particularly productive environments due to seasonal upwelling[93], and indeed, our estimates of cryptobenthic productivity exceeded estimates for a degraded but species-rich reef on the Australian Great Barrier Reef (GBR) (2.31 vs. 0.64 kg $ha^{-1}d^{-1}$)[94]. In contrast, even the optimistic estimate of 0.38 g $ha^{-1}d^{-1}$ for the Arabian Gulf compared poorly with the same degraded GBR-reef. Notably, the study site on the GBR had undergone a sequence of severe disturbances[94], which greatly reduced space and shelter availability for small-bodied

fishes; yet, it retained a diverse assemblage of cryptobenthic fish species that were likely able to satisfy their energetic demands due to benign temperature profiles[30]. At the time of our survey, reefs in the Arabian Gulf had undergone extensive bleaching in previous years[95–98], which may have negatively affected the diversity and abundance of cryptobenthic fishes compared to the less disturbed reefs in the Gulf of Oman[28,99,100]. However, the lack of difference in benthic community structure observed between regions suggests that benthic structure was not a primary driver of the observed patterns. Although the loss of some specialist cryptobenthic species has been reported after substantial live coral cover loss[95,101], previous studies have not detected substantial short-term changes in either small reef fish richness and abundance or in overarching ecosystem productivity[31,33,57,95].

Our results showcase an imminent threat to cryptobenthic reef fishes and their critical role for coral reef functioning: similar to corals, which are highly susceptible to extreme temperatures[27], many of the world's smallest marine ectotherms may struggle to compensate for increasing growth costs as they adapt to warming temperatures. As a consequence, small consumer productivity, energy transfer, and replenishment of biomass at the bottom of the fish food chain may severely decrease under climate change[18]. Analogous to cryptobenthics, the Arabian Gulf harbors less diverse and abundant communities of large reef fishes compared to nearby locations with more moderate temperatures[102,103]. It remains unresolved whether these patterns are driven by similar mechanisms as proposed herein (e.g., the energetic filtering effect on large fish species) or relate to decreased productivity at lower trophic levels. Yet, in light of the hypothesized importance of small vertebrate consumers in global food webs[104] and

463 the unique ecological role of cryptobenthics in coral reef trophic dynamics[54], the effects
464 of elevated temperature on cryptobenthic fish assemblages may considerably reduce
465 ecosystem functioning on future coral reefs.
466
467 **Methods:**
468 We studied cryptobenthic fish communities across six distinct coral reefs in two distinct
469 locations that dramatically differ in yearly temperature fluctuations. Sampled reefs in the
470 Arabian Gulf (Dhabiya: 24.36383º, 54.10121º; Ras Ghanada: 24.84743º, 54.69235º;
471 Saadiyat: 24.65771º, 54.48691º) are some of the most extreme reefs in the world in
472 terms of the annual temperature gradient, with summer maximum temperatures
473 reaching up to or above 36 ºC, while winter minimum temperatures fall to 16 ºC. In
474 contrast, sampled reefs in the Gulf of Oman (Dibba Rock: 25.55378º, 56.35694º; Sharm
475 Rock: 25.48229º, 56.36695º; Snoopy Rock: 25.49210º, 56.36401º) lie within more
476 typical coral reef temperature profiles throughout the year, ranging from 32 ºC to 22 ºC.
477 All fieldwork was performed in April and May of 2018.
478
479 *Field sampling*
480 We sampled six distinct reefs (hereafter *site*) in the southeastern Arabian Gulf and
481 northwestern Gulf of Oman (three sites per location). At each site, we sampled three
482 distinct reef outcrops for cryptobenthic reef fishes using enclosed clove oil stations[51,105],
483 covering an average of 4.63 ± 0.38 and 4.73 ± 0.16 m^2 in the Arabian Gulf and Gulf of
484 Oman, respectively, for a total of 18 community samples. For each station, we covered
485 a reef outcrop with a fine-mesh, bell-shaped net (2.74 m in diameter), weighted by a

chain on the bottom. We then covered the same area with an impermeable bell-shaped tarpaulin, also weighted by a chain on the bottom. Then, three to four divers inoculated the area under the net with two liters of clove-oil:ethanol solution (1:5) using collapsible spray bottles (clove bud oil: Jedwards International, Inc., Braintree, MA, USA). Upon emptying the entire solution and a short wait period to allow the clove oil to disperse and take effect (approximately 2-3 mins), we removed the tarpaulin and gently peeled back the net while collecting all fishes found within the inoculated area with tweezers. We searched the entire area, including inside caves and crevices until five minutes passed without a single diver collecting any additional fishes. We placed all fishes into Ziplock bags, brought them to the surface, euthanized them with a clove-oil overdose, and immediately placed them into an ice-water slurry until processing and preservation. At the end of each day, all specimens were brought to the laboratory at NYUAD or to room #211 at the Radisson Blu hotel in Fujairah. To quantify benthic community structure, we used a haphazardly placed 20×20cm PVC-quadrat to frame and take five photographs of the benthos at each sampled outcrop.

In addition to the quantitative samples obtained from the clove-oil stations, we collected cryptobenthic fish individuals for thermal tolerance trials using roving diver collections. Specifically, two divers, each equipped with spray bottles of clove-oil:ethanol solution, a dipnet, and Ziplock bags, searched the reef for cryptobenthic fishes across three species in the Arabian Gulf (*Coryogalops anomolus*, *Ecsenius pulcher*, and *Enneapterygius ventermaculus*) and six species in the Gulf of Oman (*C. anomolus*, *E. pulcher*, and *E. ventermaculus* plus *Eviota guttata*, *Helcogramma fuscopinna*, and *Hetereleotris vulgaris*). Upon locating an individual or identifying a

suitable microhabitat in which a fish was suspected, the diver applied the clove-oil solution until the fish showed signs of anesthesia. At the earliest opportunity, we caught the fish with a dipnet and placed it into a ziplock bag. Upon completion of the dive, all fishes were placed in small holding tanks equipped with air stones and periodically replenished with fresh seawater. Upon completion of all collections, fishes were brought to the seawater laboratory facilities at NYUAD. All roving diver collections were performed at Dhabiya Reef (Arabian Gulf) and Snoopy Rock (Gulf of Oman).

Laboratory processing

For samples obtained from the enclosed clove-oil stations, we followed an established protocol that involved photographing, identifying, recording, measuring, weighing and preserving each specimen[51]. To photograph the fishes, we placed each individual in a small photo tank and used a Nikon D300 DSLR camera with an AF-S Micro Nikkor 60mm macro lens (f/2.8G ED; Nikon Inc., Melville, NY, USA) against a black or white background. We measured each individual to the nearest 0.1mm using digital calipers and weighed the individual (wet weight) to the nearest 0.001 grams on a precision jewelry scale. We preserved all individuals in 95% ethanol, either separately or in lots with conspecifics. A subset of the samples was shipped to the University of Washington Fish Collection, where they were cataloged, while the rest were retained and archived at NYUAD.

Benthic photo analysis

For the benthic photographs, we created a grid with 16 equally spaced points which we superimposed on every photograph. We then categorized the benthos at each of the points into functional groups, including barnacles, bleached corals, crustose coralline algae, dead coral, hydroids, branching, encrusting, foliose, and massive live coral, mollusks, bare rock, soft sediment, sponges, algal turf, and sea urchins. Whenever visual identification was not possible (due to obstruction, shading, or blurriness), we categorized the point as “unidentifiable” (n = 69 out of 1,440). All photographs with the grid superimposed will be made accessible with the raw data of the paper.

Critical thermal maximum and minimum trials

We examined individual temperature tolerances by using critical thermal maximum (CT_{max}) and minimum (CT_{min}) trials[106]. We transported all fishes caught during roving diver collections to the wet laboratory facilities at NYUAD and housed them for at least 48 hours in large holding tanks. Trials took place from the 9th to 13th of May of 2018. For the trials, a haphazardly selected subset of individuals was moved from the holding tanks into separate chambers filled with seawater at ambient temperature and salinity. Then, after providing individuals with a 15-minute settlement period, we incrementally decreased (CT_{min}) or increased (CT_{max}) the water temperature within the chambers while keeping all other parameters constant. Specifically, we lowered or increased the temperature by 0.1º C every minute[106] while keeping all fishes under constant observation. Critical endpoints were classified as loss of equilibrium or uncontrolled swimming without a righting response for two seconds or more[106]. When individuals reached their critical endpoints, they were immediately removed, euthanized with a

clove-oil overdose, measured, weighed, and photographed. In total, we processed 60 individuals across six species for CT_{max} trials, and 62 individuals across the same species for CT_{min} trials.

Gut content DNA metabarcoding

We processed a subset of individuals across six species (*A. adenensis*, *C. anomolus*, *E. pulcher*, *E. guttata*, *E. ventermaculus*, and *H. vulgaris*) for gut content DNA metabarcoding at the University of Washington. We haphazardly selected ten, ten, and seven (due to limited sample availability) individuals of *C. anomolus*, *E. ventermaculus*, and *E. pulcher*, respectively, from the Arabian Gulf, and ten individuals each (with the exception of *E. pulcher*, for which we selected eleven individuals) of *C. anomolus*, *E. ventermaculus, A. adenensis*, *E. guttata,* and *H. vulgaris* from the Gulf of Oman. Then, under sterile conditions, we dissected out the entire alimentary tract and removed all other organs (e.g. liver, gonads) under a Zeiss V20 SteREO dissecting microscope using micro-surgery tools. We placed the entire gut into an extraction tube and performed DNA extractions with a DNeasy PowerSoil Pro DNA Isolation Kit (Qiagen, Hilden, Germany). We stored all DNA extracts at 4º C until further processing.

All DNA samples were sent to Jonah Ventures (Boulder, Colorado, USA) for two-step PCRs, library preparation, and sequencing. We targeted two universal gene regions: the mitochondrial cytochrome c oxidase subunit I (COI) for metabarcoding metazoan biodiversity and the chloroplast 23S rRNA for metabarcoding algae. For the COI gene, we selected the m1COIintF forward primer[107] and jgHCO2198 reverse primer[108]. For the 23S gene, we selected the p23SrV_f1 and Diam23Sr1 23S

primers[109–111]. All COI and 23S primers contained a 5' adaptor sequence to facilitate indexing and sequencing. The PCR reactions for both COI and 23S genes were run at a volume of 25 μl according to the Promega PCR Master Mix guidelines (Promega, Madison, Wisconsin, USA): 12.5 μl Master Mix, 0.5 μM of each primer, 1 μl gDNA, and 10.5 μl DNase/Rnase-free water. For COI, PCR amplification was run with the following conditions: initial denaturation at 94 °C for 2 minutes, followed by 45 cycles of 15 seconds at 94 °C, 30 seconds at 50 °C, and 1 minute at 72 °C, then a final elongation at 72 °C for 10 minutes. For 23S, DNA was PCR-amplified under the following conditions: initial denaturation at 94 °C for 3 minutes, followed by 40 cycles of 30 seconds at 94 °C, 45 seconds at 55 °C, and 1 minute at 72 °C, then a final elongation at 72 °C for 10 minutes. After PCR amplification, each reaction was visually inspected with a 2% agarose gel to ensure successful amplification and determine amplicon size.

All remaining library preparation and sequencing protocols apply to both the COI and 23S markers. Clean-ups were performed by incubating amplicons with Exo1/SAP for 30 minutes at 37 °C, followed by inactivation at 95 °C for 5 minutes, then the products were stored at -20 °C. Next, a second indexing PCR was performed to bind a unique 12-nucleotide index sequence. The PCR reaction included Promega Master mix, 0.5 μM of each primer, and 2 μl of template DNA. The PCR was performed with the following conditions: initial denaturation at 95 °C for 3 minutes, followed by 8 cycles of 95 °C for 30 seconds, 55 °C for 30 seconds, and 72 °C for 30 seconds. Each reaction was visually inspected with a 2% agarose gel to ensure successful amplification.

25 μl of each indexed amplicon was cleaned and normalized with the SequalPrep Normalization Kit (Life Technologies, Carlsbad, California, USA) according to the

manufacturer's protocol. For sample pooling, 5 μl of each sample was added together. Finally, library pools were sent to the Genohub service provider (Austin, Texas, USA). Prior to sequencing, quality control measures were performed, including bead cleaning with Agencourt AMPure XP beads (Beckman Coulter, Brea, California, USA) to remove <200 bp amplicons, sample quantification with a Qubit Fluorometer (Invitrogen, Carlsbad, California, USA), and amplicon average size analysis with an Agilent TapeStation 4200 (Agilent, Santa Clara, California, USA). Finally, sequencing was performed on an Illumina HiSeq using the HiSeq Rapid SBS Kit v2, 500-cycles (Illumina, San Diego, California, USA).

Sequence bioinformatics

For the COI sequences, a joint QIIME[112] and UPARSE[113] pipeline was employed for bioinformatic processing. Sequences were demultiplexed and initial quality filtering was performed with QIIME v1.9.1. Primer sequences were trimmed with Cutadapt v1.18[114], then forward and reverse reads were pair-end merged with USEARCH v11.0.667[115]. Quality filtering was then performed in accordance with the UPARSE pipeline. Sequences were clustered into operational taxonomic units (OTUs) at 99% similarity, and the OTU table was generated by mapping quality-filtered reads back to the OTU seeds. Taxonomy was assigned to OTUs by recording the top basic local alignment search tool (BLASTn[116]) hit when query coverage and percent identity exceeded 95% and 80%, respectively. GenBank was used as the reference database. When OTU taxonomic assignments did not meet these criteria, taxonomy was removed and recorded as "NA." Finally, we removed all self-hits from the OTU-dataset, which we

identified by matching the highest sequence reads of each species to its individuals, as well as unambiguous (>97% identity match) assignments to species not found in the geographic region (specifically *Oncorhynchus nerka*).

For the 23S sequences, raw sequences were processed with the JAMP pipeline (https://github.com/VascoElbrecht/JAMP). After demultiplexing, forward and reverse reads were pair-end merged with USEARCH v11.0.667[115]. Primers were trimmed from both ends using Cutadapt v1.18[114], and quality filtering was conducted with expected error filtering, as implemented through USEARCH[117]. Reads affected by sequencing and PCR error were removed using the UNOISE algorithm[118]. Exact sequence variants (ESVs) were then compiled into an ESV table, which included read counts for each sample. Taxonomy was assigned to each ESV by mapping them against a 23S database from Silva[119], specifying zero deviations to ensure mapping accuracy. Consensus taxonomy was generated from the hit tables, first considering 100% matches, then decreasing by 1% until hits were available for each ESV. Taxonomy that was present in at least 90% of the hits was reported; otherwise, an “NA” was assigned when several different taxa matched the ESV. For error reduction due to misidentified taxa, the bracket was increased to 2% when matches of 97% and higher were present, but no family-level or lower taxonomy was assigned.

Data analyses and modeling

To analyze the community variables, we first calculated the surface area (*SA*) for each sampled outcrop from the curved surface length (*CSL*) by deriving the sampled outcrop’s radius *r* ($r = 2*CSL/2\pi$), then computing available surface area under the

646 assumption that outcrops are hemispherical constructs ($SA = 4\pi r_2/2$). We calculated the
647 sum of individuals, species, and their respective body weight for each station to obtain
648 abundance, diversity, and biomass estimates, which we converted to density estimates
649 by dividing them by the sampled surface area. Using these estimates, we performed
650 three Bayesian hierarchical models, each on the natural logarithm of the response
651 variables (species density, individual density, and biomass per m_2). Models were
652 specified to include the fixed effect of *Location* (*Arabian Gulf vs. Gulf of Oman*) and the
653 random effect of *Site* (*Dhabiya*, *Ras Ghanada*, *Saadiyat*, *Dibba Rock*, *Sharm Rock*,
654 *Snoopy Rock*) and were run with a Gaussian error distribution. For each model, we ran
655 four chains with 4,000 post burn-in samples, and we validated chain convergence
656 visually. We used the default, non-informative priors set by the *brm* function in the *brms*
657 R package[120]. Then, we used the model parameters to predict distributions based on
658 1,000 draws from the posterior and plotted the distributions, their mean and confidence
659 bands, and the raw data for each site to evaluate model fit.
660 To examine cryptobenthic fish community composition across the two locations,
661 we created a species-by-sample matrix indicating the abundance of each species in a
662 given sample. We then performed a non-metric multidimensional scaling (nMDS)
663 ordination with the Bray-Curtis dissimilarity matrix of the data in two dimensions (stress
664 = 0.101). We performed a permutational analysis of variance (PERMANOVA) on the
665 same distance matrix (using 999 permutations) and extracted the most influential
666 species using the similarity of percentages (SIMPER) routine. We constructed convex
667 hull polygons for the two locations (as determined by the location of each sample) and
668 plotted them in a biplot with the seven most influential species (average contribution >

669 0.025) superimposed. For benthic community composition, we followed a similar
670 process. After our initial categorization, we first combined live coral categories into
671 “branching” and “other” and omitted all categories with fewer than three records
672 (bleached coral and hydroids) from the data. We also excluded the “unidentifiable”
673 category (<5% of points). We then calculated the proportional contribution of each
674 category to the benthos in a given sampled outcrop and arranged the data into a
675 sample-by-category matrix and performed another nMDS analysis as per above. We
676 also performed a PERMANOVA and visualized the data in the same way as described
677 above, but we did not perform the SIMPER routine due to the lower number of
678 categories. Further, we scaled the size of the symbols to represent the percent of live
679 coral cover. Finally, we statistically compared live coral cover among the two locations
680 using a Bayesian hierarchical model. We logit-transformed proportional *LiveCoralCover*
681 and specified *Location* as a fixed effect, with *Site* specified as a random effect. Model
682 and chain specifications were programmed as described above.
683 To compare intrinsic temperature tolerances, as derived from CT_{min} and CT_{max}
684 trials, we ran two separate Bayesian linear models. For both models, we specified an
685 effect of *Population* (i.e., separate levels for each species and their respective Arabian
686 Gulf and Gulf of Oman populations) on the critical thermal limit of individuals and
687 examined differences between pairwise levels using post-hoc contrasts (Tables S2 and
688 S3). Models were run with a Gaussian error distribution and the same specifications as
689 the previous models (e.g., burnin, iterations, priors, etc.). We took 1,000 draws from the
690 posterior parameters to fit posterior distributions as well as their mean and confidence
691 bands and plotted them alongside the raw data. Furthermore, to examine location-

692 specific differences in length-weight relationships and species-specific abundances, we
693 isolated individuals from three species (*C. anomolus*, *E. pulcher*, and *E. ventermaculus*)
694 and ran separate models for each species to test the effects of total length (*TL*) and
695 *Location* on *Weight*, with log-transformations of both *Weight* and *TL* and the effect of
696 location (with a random effect of *Site*) on abundance. We used a Gaussian error
697 distribution for the first set of models since the data were continuous and approximately
698 normally distributed. We used a negative binomial error distribution for the second set of
699 models since the data were non-negative integers and over-dispersed when run under a
700 Poisson distribution. To validate the model performance, we used the posterior
701 parameters to predict values across a sequence of 100 evenly spaced values within the
702 sampled size range of the two populations. We performed this 500 times and plotted
703 each predicted model fit alongside the raw data. Models were run with the same prior
704 and chain specifications as detailed above.
705 We examined prey item ingestion of the examined fishes using a network theory
706 approach for both the COI and 23S markers[121]. We first created a presence-absence
707 matrix of OTUs/ESVs across fish individuals in all species and their populations,
708 creating a bipartite dietary network based on prey presence or absence. To examine the
709 community structure within the network, we omitted all prey items with only a single
710 occurrence across the dataset since the full dataset identified the majority of individuals
711 as unique modules. This step reduced the COI dataset from 1,357 to 1,046 unique
712 predator-prey interactions and the 23S dataset from 7,872 to 5,698 predator-prey
713 interactions. We then sought to identify modules within the network using Newman's
714 modularity measure[122]. We used Beckett's community detection algorithm[123], which we

715 re-iterated 20 times for each dataset. We then used the convergent output from the 20
716 iterations to determine the module membership of each individual in our network. We
717 then created a data frame from the original presence-absence matrix that contained
718 each OTU/ESV and its linkage to the fish individual in two columns, which we then
719 summarized by the respective modules. This created a list of symbolic edges in the
720 network across the two columns, linking each prey item to a module, which we plotted
721 as a bipartite dietary network tree using the Fruchterman-Reingold algorithm. We also
722 plotted module membership in a mosaic plot.
723 Furthermore, for the COI and 23S markers, we investigated prey item diversity
724 ingested by each species' population by producing interpolated and extrapolated
725 rarefaction curves, which showcase sequencing depth by plotting prey item species
726 richness by the total number of sequences detected for each species. We ran
727 rarefaction analyses by rarefying species richness estimates for each species or
728 population to an endpoint defined by the maximum sequences in any population using
729 100 bootstraps and 50 knots along the x-axis[124].
730 Finally, we modelled growth and mortality dynamics in cryptobenthic fish
731 assemblages from the two locations, ultimately yielding a standing biomass estimate
732 and three rate-based metrics that serve as indicators of energy and nutrient fluxes, thus
733 indicating ecosystem functioning[25]: produced biomass (in g $d^{-1}m^{-2}$), consumed biomass
734 (in g $d^{-1}m^{-2}$), and total turnover (percent d^{-1})[94,125,126]. Produced biomass represents the
735 amount of fish tissue accumulated by an assemblage (in this case, a cryptobenthic fish
736 assemblage collected in a given sample), thus considering only the growth that will
737 occur on any given day (based on yearly averages in this case). Consumed biomass

738 represents the amount of fish tissue that perished based on our estimates of fish
739 mortality. In this pathway, the energy and nutrients produced by fishes are provided to
740 other consumers or decomposers via predation or detritivory. Finally, total turnover
741 expands on the classic estimate of turnover (the production/standing biomass [P/B]
742 ratio[127]) by also including consumed biomass (consumed biomass/standing biomass)[125].
743 As such, the turnover metric approximates the rate at which particles flow through the
744 system, either via incorporation into fish biomass or release to other consumers through
745 mortality.

746 For the modeling, we first accrued species-specific information on maximum
747 lengths and a range of coarse ecological traits (pertaining to diet, sociality, habitat
748 association, and prevailing mean sea surface temperatures [SST]) from the literature for
749 each species in our samples. We also extracted length-weight relationships at the
750 family-level, since not all species in our samples were common enough to construct
751 robust length-weight relationships. We then used these data to calculate species-
752 specific growth coefficients (K_{max}) to the specified maximum size and modeled individual
753 weight gain based on changes in fish size per day under a Von Bertalanffy Growth
754 Model (VBGM)[126]. By subtracting the observed fish size (as obtained from our samples)
755 from the weight obtained by the same fish after one day (from the model), we calculated
756 the expected biomass production by that individual. We estimated daily mortality rates
757 by calculating species-level mortality risk coefficients via VBGM parameters and
758 SST[125,128], and then we adjusted the risk based on relationships between mortality and
759 body size[129]. Using these coefficients, we obtained a daily survival probability for a
760 given individual in the dataset. By combining this probability with biomass production as

obtained from the previous step, we were able to generate the expected loss of biomass due to natural mortality at the individual level. Finally, we summed the individual-level estimates of weight, growth, and mortality for each sample to obtain community-level values of standing biomass, produced biomass, and consumed biomass, which we used to calculate total turnover as the combined quotients of produced and consumed biomass and standing biomass.

All data preparation, analyses, and visualizations were performed in *R*[130] (version 3.6.1) using the *tidyverse*[131], *vegan*[132], *brms*[120], *iNEXT*[124], *igraph*[133], *bipartite*[134], *tidybayes*[135], *xgboost*[136], *emmeans*[137], *oceanmap*[138], *ncdf4*[139] and *raster*[140] packages. All graphs were made using the *Trimma lantana* and *Coryphaena hippurus* color palettes in the package *fishualize*[141]. Growth modeling was performed using a beta version of the package *rfishprod*.

References

1. Dornelas, M. *et al.* Assemblage time series reveal biodiversity change but not systematic loss. *Science* **344**, 296–299 (2014).
2. Blowes, S. A. *et al.* The geography of biodiversity change in marine and terrestrial assemblages. *Science* **366**, 339–345 (2019).
3. Johnson, C. N. *et al.* Biodiversity losses and conservation responses in the Anthropocene. *Science* **356**, 270–275 (2017).
4. Mace, G. M., Norris, K. & Fitter, A. H. Biodiversity and ecosystem services: a multilayered relationship. *Trends in ecology & evolution* **27**, 19–26 (2012).
5. Vellend, M. *The theory of ecological communities (MPB-57)*. vol. 75 (Princeton University Press, 2016).
6. Kraft, N. J. *et al.* Community assembly, coexistence and the environmental filtering metaphor. *Functional Ecology* **29**, 592–599 (2015).
7. Kraft, N. J., Valencia, R. & Ackerly, D. D. Functional traits and niche-based tree community assembly in an Amazonian forest. *Science* **322**, 580–582 (2008).
8. Leibold, M. A. *et al.* The metacommunity concept: a framework for multi-scale community ecology. *Ecology letters* **7**, 601–613 (2004).
9. Cardinale, B. J. *et al.* Biodiversity loss and its impact on humanity. *Nature* **486**, 59–67 (2012).
10. Duffy, J. E., Godwin, C. M. & Cardinale, B. J. Biodiversity effects in the wild are common and as strong as key drivers of productivity. *Nature* **549**, 261 (2017).
11. Schweiger, A. K. *et al.* Plant spectral diversity integrates functional and phylogenetic components of biodiversity and predicts ecosystem function. *Nature ecology & evolution* **2**, 976 (2018).
12. Pecl, G. T. *et al.* Biodiversity redistribution under climate change: Impacts on ecosystems and human well-being. *Science* **355**, eaai9214 (2017).
13. Scheffers, B. R. *et al.* The broad footprint of climate change from genes to biomes to people. *Science* **354**, aaf7671 (2016).
14. García, F. C., Bestion, E., Warfield, R. & Yvon-Durocher, G. Changes in temperature alter the relationship between biodiversity and ecosystem functioning. *Proceedings of the National Academy of Sciences* **115**, 10989–10994 (2018).
15. Pörtner, H. O. & Farrell, A. P. Physiology and climate change. *Science* **322**, 690–692 (2008).
16. Deutsch, C., Ferrel, A., Seibel, B., Pörtner, H.-O. & Huey, R. B. Climate change tightens a metabolic constraint on marine habitats. *Science* **348**, 1132–1135 (2015).
17. Bozinovic, F. & Pörtner, H. Physiological ecology meets climate change. *Ecology and evolution* **5**, 1025–1030 (2015).
18. Barneche, D. R., Jahn, M. & Seebacher, F. Warming increases the cost of growth in a model vertebrate. *Functional Ecology*.
19. Brown, J. H., Hall, C. A. & Sibly, R. M. Equal fitness paradigm explained by a trade-off between generation time and energy production rate. *Nature ecology & evolution* **2**, 262 (2018).
20. Toseland, A. *et al.* The impact of temperature on marine phytoplankton resource allocation and metabolism. *Nature Climate Change* **3**, 979 (2013).
21. Barneche, D. R. & Allen, A. P. The energetics of fish growth and how it constrains food-web trophic structure. *Ecology letters* **21**, 836–844 (2018).
22. Gardner, J. L., Peters, A., Kearney, M. R., Joseph, L. & Heinsohn, R. Declining body size: a third universal response to warming? *Trends in ecology & evolution* **26**, 285–291 (2011).
23. Chesson, P. Mechanisms of maintenance of species diversity. *Annual review of Ecology and Systematics* **31**, 343–366 (2000).
24. Barnes, A. D. *et al.* Energy flux: the link between multitrophic biodiversity and ecosystem functioning. *Trends in ecology & evolution* **33**, 186–197 (2018).

25. Brandl, S. J. *et al.* Coral reef ecosystem functioning: eight core processes and the role of biodiversity. *Frontiers in Ecology and the Environment* (2019).
26. Spalding, M. *et al.* Mapping the global value and distribution of coral reef tourism. *Marine Policy* **82**, 104–113 (2017).
27. Hughes, T. P. *et al.* Spatial and temporal patterns of mass bleaching of corals in the Anthropocene. *Science* **359**, 80–83 (2018).
28. Pratchett, M. S., Hoey, A. S., Wilson, S. K., Messmer, V. & Graham, N. A. Changes in biodiversity and functioning of reef fish assemblages following coral bleaching and coral loss. *Diversity* **3**, 424–452 (2011).
29. Brandl, S. J., Emslie, M. J. & Ceccarelli, D. M. Habitat degradation increases functional originality in highly diverse coral reef fish assemblages. *Ecosphere* **7**, (2016).
30. Fontoura, L. *et al.* Climate-driven shift in coral morphological structure predicts decline of juvenile reef fishes. *Global change biology* (2019).
31. Bellwood, D. R., Hoey, A. S., Ackerman, J. L. & Depczynski, M. Coral bleaching, reef fish community phase shifts and the resilience of coral reefs. *Global Change Biology* **12**, 1587–1594 (2006).
32. Robinson, J. P. *et al.* Productive instability of coral reef fisheries after climate-driven regime shifts. *Nature ecology & evolution* **3**, 183 (2019).
33. Wismer, S., Tebbett, S. B., Streit, R. P. & Bellwood, D. R. Young fishes persist despite coral loss on the Great Barrier Reef. *Communications Biology* **2**, 456 (2019).
34. Taylor, B. M. *et al.* Synchronous biological feedbacks in parrotfishes associated with pantropical coral bleaching. *Global Change Biology* (2019).
35. Pörtner, H. O. & Knust, R. Climate change affects marine fishes through the oxygen limitation of thermal tolerance. *science* **315**, 95–97 (2007).
36. Comte, L. & Olden, J. D. Climatic vulnerability of the world's freshwater and marine fishes. *Nature Climate Change* **7**, 718 (2017).
37. Munday, P. L., McCormick, M. I. & Nilsson, G. E. Impact of global warming and rising CO2 levels on coral reef fishes: what hope for the future? *Journal of Experimental Biology* **215**, 3865–3873 (2012).
38. Munday, P. L., Jones, G. P., Pratchett, M. S. & Williams, A. J. Climate change and the future for coral reef fishes. *Fish and Fisheries* **9**, 261–285 (2008).
39. Donelson, J., Munday, P., McCormick, M. & Pitcher, C. Rapid transgenerational acclimation of a tropical reef fish to climate change. *Nature Climate Change* **2**, 30 (2012).
40. Johansen, J. & Jones, G. Increasing ocean temperature reduces the metabolic performance and swimming ability of coral reef damselfishes. *Global Change Biology* **17**, 2971–2979 (2011).
41. Rummer, J. L. *et al.* Life on the edge: thermal optima for aerobic scope of equatorial reef fishes are close to current day temperatures. *Global change biology* **20**, 1055–1066 (2014).
42. Nilsson, G. E., Crawley, N., Lunde, I. G. & Munday, P. L. Elevated temperature reduces the respiratory scope of coral reef fishes. *Global Change Biology* **15**, 1405–1412 (2009).
43. Eme, J. & Bennett, W. A. Critical thermal tolerance polygons of tropical marine fishes from Sulawesi, Indonesia. *Journal of Thermal Biology* **34**, 220–225 (2009).
44. Gardiner, N. M., Munday, P. L. & Nilsson, G. E. Counter-gradient variation in respiratory performance of coral reef fishes at elevated temperatures. *PLoS One* **5**, e13299 (2010).
45. Mora, C. & Ospina, A. Tolerance to high temperatures and potential impact of sea warming on reef fishes of Gorgona Island (tropical eastern Pacific). *Marine Biology* **139**, 765–769 (2001).
46. Feary, D. A. *et al.* Latitudinal shifts in coral reef fishes: why some species do and others do not shift. *Fish and Fisheries* **15**, 593–615 (2014).
47. Bernal, M. A. *et al.* Phenotypic and molecular consequences of stepwise temperature increase across generations in a coral reef fish. *Molecular Ecology* **27**, 4516–4528 (2018).
48. Grenchik, M., Donelson, J. & Munday, P. Evidence for developmental thermal acclimation in the damselfish, Pomacentrus moluccensis. *Coral Reefs* **32**, 85–90 (2013).

49. Miller, D. D., Ota, Y., Sumaila, U. R., Cisneros-Montemayor, A. M. & Cheung, W. W. Adaptation strategies to climate change in marine systems. *Global change biology* **24**, e1–e14 (2018).
50. Brandl, S. J., Goatley, C. H., Bellwood, D. R. & Tornabene, L. The hidden half: ecology and evolution of cryptobenthic fishes on coral reefs. *Biological Reviews* **93**, 1846–1873 (2018).
51. Brandl, S. J., Casey, J. M., Knowlton, N. & Duffy, J. E. Marine dock pilings foster diverse, native cryptobenthic fish assemblages across bioregions. *Ecology and evolution* **7**, 7069–7079 (2017).
52. Ahmadia, G. N., Tornabene, L., Smith, D. J. & Pezold, F. L. The relative importance of regional, local, and evolutionary factors structuring cryptobenthic coral-reef assemblages. *Coral Reefs* **37**, 279–293 (2018).
53. Coker, D. J., DiBattista, J. D., Sinclair-Taylor, T. H. & Berumen, M. L. Spatial patterns of cryptobenthic coral-reef fishes in the Red Sea. *Coral Reefs* 1–7 (2017).
54. Brandl, S. J. *et al.* Demographic dynamics of the smallest marine vertebrates fuel coral reef ecosystem functioning. *Science* **364**, 1189–1192 (2019).
55. Miller, P. J. Miniature vertebrates. The implications of small body size. in vol. 69 (Oxford University Press, 1996).
56. Depczynski, M. & Bellwood, D. Microhabitat utilisation patterns in cryptobenthic coral reef fish communities. *Marine Biology* **145**, 455–463 (2004).
57. Bellwood, D. R. *et al.* Coral recovery may not herald the return of fishes on damaged coral reefs. *Oecologia* **170**, 567–573 (2012).
58. Depczynski, M. & Bellwood, D. R. Shortest recorded vertebrate lifespan found in a coral reef fish. *Current Biology* **15**, R288–R289.
59. Tornabene, L., Valdez, S., Erdmann, M. & Pezold, F. Support for a 'Center of Origin'in the Coral Triangle: Cryptic diversity, recent speciation, and local endemism in a diverse lineage of reef fishes (Gobiidae: Eviota). *Molecular phylogenetics and evolution* **82**, 200–210 (2015).
60. Price, A., Sheppard, C. & Roberts, C. The Gulf: its biological setting. *Marine Pollution Bulletin* **27**, 9–15 (1993).
61. Riegl, B. M. & Purkis, S. J. Coral reefs of the Gulf: adaptation to climatic extremes in the world's hottest sea. in *Coral reefs of the Gulf* 1–4 (Springer, 2012).
62. Eagderi, S., Fricke, R., Esmaeili, H. & Jalili, P. Annotated checklist of the fishes of the Persian Gulf: Diversity and conservation status. *Iranian Journal of Ichthyology* **6**, 1–171 (2019).
63. Casey, J. M. *et al.* Reconstructing hyperdiverse food webs: Gut content metabarcoding as a tool to disentangle trophic interactions on coral reefs. *Methods in Ecology and Evolution* **10**, 1157–1170 (2019).
64. Depczynski, M. & Bellwood, D. R. The role of cryptobenthic reef fishes in coral reef trophodynamics. *Marine Ecology Progress Series* **256**, 183–191 (2003).
65. Pratchett, M. S., Wilson, S. K. & Munday, P. L. 13 Effects of climate change on coral reef fishes. *Ecology of fishes on coral reefs* 127 (2015).
66. Purkis, S. J. & Riegl, B. M. Geomorphology and Reef Building in the SE Gulf. in *Coral Reefs of the Gulf: Adaptation to Climatic Extremes* (eds. Riegl, B. M. & Purkis, S. J.) 33–50 (Springer Netherlands, 2012). doi:10.1007/978-94-007-3008-3_3.
67. Krupp, F. & Müller, T. The status of fish populations in the northern Arabian Gulf two years after the 1991 Gulf War oil spill. *Courier Forschungsinst Senckenb* **166**, 67–75 (1994).
68. Bishop, J. History and current checklist of Kuwait's ichthyofauna. *Journal of Arid Environments* **54**, 237–256 (2003).
69. Donelson, J. M., Munday, P. L., McCORMICK, M. I. & Nilsson, G. E. Acclimation to predicted ocean warming through developmental plasticity in a tropical reef fish. *Global Change Biology* **17**, 1712–1719 (2011).
70. Ohlberger, J. Climate warming and ectotherm body size–from individual physiology to community ecology. *Functional Ecology* **27**, 991–1001 (2013).

71. Peig, J. & Green, A. J. The paradigm of body condition: a critical reappraisal of current methods based on mass and length. *Functional Ecology* **24**, 1323–1332 (2010).
72. Sullam, K. E. *et al.* Changes in digestive traits and body nutritional composition accommodate a trophic niche shift in Trinidadian guppies. *Oecologia* **177**, 245–257 (2015).
73. Whelan, C. J., Brown, J. S., Schmidt, K. A., Steele, B. B. & Willson, M. F. Linking consumer–resource theory and digestive physiology: application to diet shifts. *Evolutionary Ecology Research* **2**, 911–934 (2000).
74. Petchey, O. L. Prey diversity, prey composition, and predator population dynamics in experimental microcosms. *Journal of Animal Ecology* **69**, 874–882 (2000).
75. Merrick, R. L., Chumbley, M. K. & Byrd, G. V. Diet diversity of Steller sea lions (Eumetopias jubatus) and their population decline in Alaska: a potential relationship. *Can. J. Fish. Aquat. Sci.* **54**, 1342–1348 (1997).
76. Hondorp, D. W., Pothoven, S. A. & Brandt, S. B. Influence of Diporeia density on diet composition, relative abundance, and energy density of planktivorous fishes in southeast Lake Michigan. *Transactions of the American fisheries Society* **134**, 588–601 (2005).
77. Shraim, R. *et al.* Environmental Extremes Are Associated with Dietary Patterns in Arabian Gulf Reef Fishes. *Frontiers in Marine Science* **4**, 285 (2017).
78. Agorreta, A. *et al.* Molecular phylogenetics of Gobioidei and phylogenetic placement of European gobies. *Molecular Phylogenetics and Evolution* **69**, 619–633 (2013).
79. Thacker, C. E. & Roje, D. M. Phylogeny of Gobiidae and identification of gobiid lineages. *Systematics and Biodiversity* **9**, 329–347 (2011).
80. Kovačić, M., Bogorodsky, S. V. & Mal, A. O. Two new species of Coryogalops (Perciformes: Gobiidae) from the Red Sea. *Zootaxa* **3881**, 513–531 (2014).
81. Rishworth GM, Strydom NA & Perissinotto R. Fishes associated with living stromatolite communities in peritidal pools: predators, recruits and ecological traps. *Mar Ecol Prog Ser* **580**, 153–167 (2017).
82. Munday, P. L. & Jones, G. P. The ecological implications of small body size among coral-reef fishes. *Oceanogr Mar Biol Annu Rev* **36**, 373–411 (1998).
83. Sandblom, E. *et al.* Physiological constraints to climate warming in fish follow principles of plastic floors and concrete ceilings. *Nature communications* **7**, 11447 (2016).
84. Norin, T. & Metcalfe, N. B. Ecological and evolutionary consequences of metabolic rate plasticity in response to environmental change. *Philosophical Transactions of the Royal Society B* **374**, 20180180 (2019).
85. Sheldon, K. S., Yang, S. & Tewksbury, J. J. Climate change and community disassembly: impacts of warming on tropical and temperate montane community structure. *Ecology Letters* **14**, 1191–1200 (2011).
86. Crossland, C., Hatcher, B. & Smith, S. Role of coral reefs in global ocean production. *Coral reefs* **10**, 55–64 (1991).
87. Gove, J. M. *et al.* Near-island biological hotspots in barren ocean basins. *Nature communications* **7**, 10581 (2016).
88. De Goeij, J. M. *et al.* Surviving in a marine desert: the sponge loop retains resources within coral reefs. *Science* **342**, 108–110 (2013).
89. Wild, C. *et al.* Coral mucus functions as an energy carrier and particle trap in the reef ecosystem. *Nature* **428**, 66–70 (2004).
90. Hamner, W., Jones, M., Carleton, J., Hauri, I. & Williams, D. M. Zooplankton, planktivorous fish, and water currents on a windward reef face: Great Barrier Reef, Australia. *Bulletin of Marine Science* **42**, 459–479 (1988).
91. Hatcher, B. G. Coral reef primary productivity: a beggar's banquet. *Trends in Ecology & Evolution* **3**, 106–111 (1988).

92. Bacon, P., Gurney, W., Jones, W., McLaren, I. & Youngson, A. Seasonal growth patterns of wild juvenile fish: partitioning variation among explanatory variables, based on individual growth trajectories of Atlantic salmon (Salmo salar) parr. *Journal of Animal Ecology* **74**, 1–11 (2005).
93. Coles, S. L. Coral species diversity and environmental factors in the Arabian Gulf and the Gulf of Oman: a comparison to the Indo-Pacific region. *Atoll Research Bulletin* (2003).
94. Morais, R. A. & Bellwood, D. R. Pelagic Subsidies Underpin Fish Productivity on a Degraded Coral Reef. *Current Biology* **29**, 1521–1527 (2019).
95. Riegl, B. Effects of the 1996 and 1998 positive sea-surface temperature anomalies on corals, coral diseases and fish in the Arabian Gulf (Dubai, UAE). *Marine biology* **140**, 29–40 (2002).
96. Riegl, B. & Purkis, S. Coral population dynamics across consecutive mass mortality events. *Global change biology* **21**, 3995–4005 (2015).
97. Burt, J., Al-Harthi, S. & Al-Cibahy, A. Long-term impacts of coral bleaching events on the world's warmest reefs. *Marine environmental research* **72**, 225–229 (2011).
98. Burt, J. A., Paparella, F., Al-Mansoori, N., Al-Mansoori, A. & Al-Jailani, H. Causes and consequences of the 2017 coral bleaching event in the southern Persian/Arabian Gulf. *Coral Reefs* **38**, 567–589 (2019).
99. Coker, D. J., Wilson, S. K. & Pratchett, M. S. Importance of live coral habitat for reef fishes. *Reviews in Fish Biology and Fisheries* **24**, 89–126 (2014).
100. Pratchett, M. S., Baird, A. H., Bauman, A. G. & Burt, J. A. Abundance and composition of juvenile corals reveals divergent trajectories for coral assemblages across the United Arab Emirates. *Marine Pollution Bulletin* **114**, 1031–1035 (2017).
101. Munday, P. L. Habitat loss, resource specialization, and extinction on coral reefs. *Global Change Biology* **10**, 1642–1647 (2004).
102. Burt, J. A. *et al.* Biogeographic patterns of reef fish community structure in the northeastern Arabian Peninsula. *ICES Journal of Marine Science* **68**, 1875–1883 (2011).
103. Feary, D. A., Burt, J. A., Cavalcante, G. H. & Bauman, A. G. Extreme Physical Factors and the Structure of Gulf Fish and Reef Communities. in *Coral Reefs of the Gulf: Adaptation to Climatic Extremes* (eds. Riegl, B. M. & Purkis, S. J.) 163–170 (Springer Netherlands, 2012). doi:10.1007/978-94-007-3008-3_9.
104. Brose, U. *et al.* Predator traits determine food-web architecture across ecosystems. *Nature ecology & evolution* **3**, 919 (2019).
105. Ackerman, J. L. & Bellwood, D. R. Reef fish assemblages: a re-evaluation using enclosed rotenone stations. *Marine Ecology-Progress Series* **206**, 227–237 (2000).
106. Beitinger, T. L., Bennett, W. A. & McCauley, R. W. Temperature tolerances of North American freshwater fishes exposed to dynamic changes in temperature. *Environmental biology of fishes* **58**, 237–275 (2000).
107. Leray, M. *et al.* A new versatile primer set targeting a short fragment of the mitochondrial COI region for metabarcoding metazoan diversity: application for characterizing coral reef fish gut contents. *Frontiers in zoology* **10**, 34 (2013).
108. Geller, J., Meyer, C., Parker, M. & Hawk, H. Redesign of PCR primers for mitochondrial cytochrome c oxidase subunit I for marine invertebrates and application in all-taxa biotic surveys. *Molecular ecology resources* **13**, 851–861 (2013).
109. Sherwood, A. R. & Presting, G. G. Universal primers amplify a 23S rDNA plastid marker in eukaryotic algae and cyanobacteria. *Journal of phycology* **43**, 605–608 (2007).
110. Hamsher, S. E., Evans, K. M., Mann, D. G., Poulíčková, A. & Saunders, G. W. Barcoding diatoms: exploring alternatives to COI-5P. *Protist* **162**, 405–422 (2011).
111. Cannon, M. *et al.* In silico assessment of primers for eDNA studies using PrimerTree and application to characterize the biodiversity surrounding the Cuyahoga River. *Scientific reports* **6**, 22908 (2016).

112. Caporaso, J. G. *et al.* QIIME allows analysis of high-throughput community sequencing data. *Nature methods* **7**, 335 (2010).
113. Edgar, R. C. UPARSE: highly accurate OTU sequences from microbial amplicon reads. *Nature methods* **10**, 996 (2013).
114. Martin, M. Cutadapt removes adapter sequences from high-throughput sequencing reads. *EMBnet. journal* **17**, 10–12 (2011).
115. Edgar, R. C. Search and clustering orders of magnitude faster than BLAST. *Bioinformatics* **26**, 2460–2461 (2010).
116. Camacho, C. *et al.* BLAST+: architecture and applications. *BMC bioinformatics* **10**, 421 (2009).
117. Edgar, R. C. & Flyvbjerg, H. Error filtering, pair assembly and error correction for next-generation sequencing reads. *Bioinformatics* **31**, 3476–3482 (2015).
118. Edgar, R. C. UNOISE2: improved error-correction for Illumina 16S and ITS amplicon sequencing. *BioRxiv* 081257 (2016).
119. Yilmaz, P. *et al.* The SILVA and "all-species living tree project (LTP)" taxonomic frameworks. *Nucleic acids research* **42**, D643–D648 (2013).
120. Bürkner, P.-C. Advanced Bayesian Multilevel Modeling with the R Package brms. *arXiv preprint arXiv:1705.11123* (2017).
121. Wasserman, S. & Faust, K. *Social network analysis: Methods and applications*. vol. 8 (Cambridge university press, 1994).
122. Newman, M. E. Modularity and community structure in networks. *Proceedings of the national academy of sciences* **103**, 8577–8582 (2006).
123. Beckett, S. J. Improved community detection in weighted bipartite networks. *Royal Society open science* **3**, 140536 (2016).
124. Hsieh, T., Ma, K. & Chao, A. iNEXT: an R package for rarefaction and extrapolation of species diversity (Hill numbers). *Methods in Ecology and Evolution* (2016).
125. Brandl, S. J. *et al.* Supplemental Materials for Demographic dynamics of the smallest marine vertebrates fuel coral reef ecosystem functioning. *Science* **364**, 1189–1192 (2019).
126. Morais, R. A. & Bellwood, D. R. Global drivers of reef fish growth. *Fish and Fisheries*.
127. Allen, K. R. Relation between production and biomass. *Journal of the Fisheries Board of Canada* **28**, 1573–1581 (1971).
128. Pauly, D. On the interrelationships between natural mortality, growth parameters, and mean environmental temperature in 175 fish stocks. *ICES Journal of Marine Science* **39**, 175–192 (1980).
129. Gislason, H., Daan, N., Rice, J. C. & Pope, J. G. Size, growth, temperature and the natural mortality of marine fish. *Fish and Fisheries* **11**, 149–158 (2010).
130. R Core Team. *R: A language and environment for statistical computing.* (2019).
131. Wickham, H. Tidyverse: Easily install and load'tidyverse'packages. *R package version* **1**, (2017).
132. Oksanen, J. *et al.* The vegan package. *Community ecology package* **10**, (2007).
133. Csardi, G. & Nepusz, T. The igraph software package for complex network research. *InterJournal, Complex Systems* **1695**, 1–9 (2006).
134. Dormann, C. F., Gruber, B. & Fründ, J. Introducing the bipartite package: analysing ecological networks. *interaction* **1**, (2008).
135. Kay, M. tidybayes: Tidy data and geoms for Bayesian models. *R package version* **1**, (2018).
136. Chen, T., He, T., Benesty, M., Khotilovich, V. & Tang, Y. Xgboost: extreme gradient boosting. *R package version 0.4-2* 1–4 (2015).
137. Lenth, R., Singmann, H., Love, J., Buerkner, P. & Herve, M. Package "emmeans": Estimated marginal means, aka least-squares means. *Compr. R Arch. Netw* 1–67 (2019).
138. Bauer, R. Oceanmap: a plotting toolbox for 2D oceanographic data. *R package, version 0.0* **9**, (2017).
139. Pierce, D. & Pierce, M. D. Package 'ncdf4'. (2019).

140. Hijmans, R. J. *et al.* Raster package in R. (2013).
141. Schiettekatte, N. M., Brandl, S. J. & Casey, J. M. *fishualize: Color palettes based on fish species*. (2019).

Acknowledgments

We thank the Environment Agency Abu Dhabi (TMBS/18/L/179) and Dibba Municipality (unnumbered) for collection permits and the UAE Ministry of Environment and Climate Change for the tissue export permit (AUD-Q-22-1110520). All work was performed under NYUAD IACUC approval 18-0003. We further thank the NYU Abu Dhabi Center for Genomics and Systems Biology for sequencing funding and the NYU Abu Dhabi Core Facilities group for support of field collections and thermal experiments. We thank Dain McParland and Grace Vaughan for field support, Noura Al-Mansoori for assistance with processing specimens in the laboratory, and Katherine Maslenikov and Jonathon Huie for assistance in cataloging specimens at the University of Washington. Partial fieldwork funding was provided to L Tornabene by the University of Washington.

Author contributions

SJB and JLJ designed the study; SJB, JLJ, JMC, and LT performed field collections; JLJ ran physiological trials; SJB, JMC, and LT performed laboratory work; JAB and LT provided funding and resources; SJB performed data analysis and visualization; SJB and RAM performed population modeling; SJB wrote the first draft of the manuscript, and all authors contributed to writing thereafter.

Data accessibility and conflicts of interest

All data and code necessary to produce the results are included in this submission and will be made public upon publication of the paper. We declare no conflict of interest.

Supplemental Material

Table S1| Presence, abundance, and previous records of species sampled in the present study. Each row represents a species, with columns *AG* (Arabian Gulf) and *GO* (Gulf of Oman) indicating the abundance of the species in our samples. Column *R* indicates whether the species has been previously recorded in other parts of the Arabian Gulf (* = yes, – = no). References for previous records are provided.

Family	***Species***	***AG***	***GO***	***R***	***Reference***
Apogonidae	*Apogon coccineus*	6	10	*	present
Apogonidae	*Apogonichthyoides taeniatus*	2	0	*	present
Apogonidae	*Cheilodipterus novemstriatus*	2	9	*	present
Apogonidae	*Cheilodipterus persicus*	0	1	*	Krupp & Müller 1994
Apogonidae	*Fowleria variegata*	5	1	*	present
Apogonidae	*Ostorhinchus cyanosoma*	0	15	*	Krupp & Müller 1994
Apogonidae	*Ostorhinchus fleurieu*	0	30	*	Eagderi et al. 2019
Batrachoididae	*Colletteichthys occidentalis*	6	0	*	present
Blenniidae	*Antennablennius adenensis*	0	54	*	Bishop 2003
Blenniidae	*Ecsenius pulcher*	8	97	*	present
Blenniidae	*Laiphognathus multimaculatus*	1	0	*	present
Bythitidae	*Dinematichthys iluocoeteoides*	5	0	*	present
Gobiidae	*Asterropteryx semipunctata*	0	2	*	Krupp & Müller 1994
Gobiidae	*Callogobius bifasciatus*	2	0	*	present
Gobiidae	*Callogobius speA*	0	3	*	Eagderi et al. 2019
Gobiidae	*Coryogalops anomalus*	65	33	*	present
Gobiidae	*Eviota guttata*	0	69	*	Krupp & Müller 1994
Gobiidae	*Eviota punyit*	0	12	*	Krupp & Müller 1994[1]
Gobiidae	*Favonigobius melanobranchus*	1	0	*	present
Gobiidae	*Fusigobius inframaculatus*	0	3	*	Eagderi et al. 2019
Gobiidae	*Gnatholepis caudimaculata*	0	14	*	Eagderi et al. 2019
Gobiidae	*Gobiodon reticulatus*	0	2	*	Bishop 2003
Gobiidae	*Hetereleotris vulgaris*	0	405	*	Eagderi et al. 2019
Gobiidae	*Istigobius decoratus*	0	15	*	Eagderi et al. 2019
Gobiidae	*Priolepis cincta*	0	4	*	Winterbottom & Burridge 1992
Gobiidae	*Priolepis randalli*	0	2	*	Winterbottom & Burridge 1993
Gobiidae	*Priolepis semidoliata*	0	10	–	NA
Gobiidae	*Trimma corallinum*	0	11	*	Eagderi et al. 2019[2]
Muraenidae	*Gymnothorax speA*	0	12	*	Eagderi et al. 2019[3]
Ostraciidae	*Ostracion cubicus*	0	3	*	Eagderi et al. 2019
Pomacanthidae	*Pomacanthus maculosus*	7	0	*	present
Pomacentridae	*Chromis flavaxilla*	0	19	*	Bishop 2003
Pomacentridae	*Chromis xanthopterygius*	0	3	*	Bishop 2003
Pomacentridae	*Neopomacentrus cyanomos*	0	38	*	Bishop 2003
Pomacentridae	*Neopomacentrus miryae*	0	38	–	NA
Pomacentridae	*Neopomacentrus sindensis*	0	6	*	Bishop 2003
Pomacentridae	*Pomacentrus aquilus*	3	0	*	present
Pomacentridae	*Pomacentrus leptus*	0	5	*	Bishop 2003
Pomacentridae	*Pomacentrus trichrourus*	5	0	*	present
Pseudochromidae	*Pseudochromis aldabraensis*	0	4	*	Bishop 2003

Pseudochromidae	*Pseudochromis linda*	1	0	*	present
Pseudochromidae	*Pseudochromis nigrovittatus*	2	1	*	present
Pseudochromidae	*Pseudochromis persicus*	1	0	*	present
Serranidae	*Cephalopholis hemistiktos*	2	2	*	present
Syngnathidae	*Corythoichthys flavofasciata*	0	5	*	Froese & Pauly 2019
Syngnathidae	*Doryrhamphus excisus*	0	3	*	Bishop 2003
Tripterygiidae	*Enneapterygius ventermaculus*	131	262	*	present
Tripterygiidae	*Helcogramma fuscopinna*	0	134	–	NA

[1]identified as *E. sebreei*
[2]synonymous with *T. winterbottomi*
[3]genus level

Table S2 | Contrasts between levels of the explanatory variable for the model testing CT_{max} differences in cryptobenthic reef fishes. Population columns highlight the contrast estimated in the model, whereas the estimate and its confidence intervals indicate estimated differences.

Population I	Population II	Estimate	LCI	UCI
C. anomolus.AG	*E. pulcher.AG*	*0.486*	*-0.079*	*1.054*
C. anomolus.AG	*E. ventermaculus.AG*	*1.360*	*0.808*	*1.949*
C. anomolus.AG	*E. pulcher.GoO*	*1.114*	*0.581*	*1.726*
C. anomolus.AG	*E. ventermaculus.GoO*	*1.633*	*0.939*	*2.342*
C. anomolus.AG	*E. guttata.GoO*	*1.143*	*0.534*	*1.759*
C. anomolus.AG	*H. fuscopinna.GoO*	*2.392*	*1.758*	*2.992*
C. anomolus.AG	*H. vulgaris.GoO*	*0.492*	*-0.061*	*1.078*
E. pulcher.AG	*E. ventermaculus.AG*	*0.879*	*0.509*	*1.252*
E. pulcher.AG	*E. pulcher.GoO*	*0.636*	*0.244*	*1.016*
E. pulcher.AG	*E. ventermaculus.GoO*	*1.159*	*0.624*	*1.737*
E. pulcher.AG	*E. guttata.GoO*	*0.656*	*0.227*	*1.134*
E. pulcher.AG	*H. fuscoguttata.GoO*	*1.905*	*1.463*	*2.341*
E. pulcher.AG	*H. vulgaris.GoO*	*0.011*	*-0.368*	*0.417*
E. ventermaculus.AG	*E. pulcher.GoO*	*-0.245*	*-0.640*	*0.118*
E. ventermaculus.AG	*E. ventermaculus.GoO*	*0.277*	*-0.260*	*0.815*
E. ventermaculus.AG	*E. guttata.GoO*	*-0.225*	*-0.680*	*0.212*
E. ventermaculus.AG	*H. fuscopinna.GoO*	*1.024*	*0.578*	*1.449*
E. ventermaculus.AG	*H. vulgaris.GoO*	*-0.878*	*-1.265*	*-0.508*
E. pulcher.GoO	*E. ventermaculus.GoO*	*0.519*	*-0.0290*	*1.073*
E. pulcher.GoO	*E. guttata.GoO*	*0.020*	*-0.426*	*0.494*
E. pulcher.GoO	*H. fuscopinna.GoO*	*1.274*	*0.839*	*1.726*
E. pulcher.GoO	*H. vulgaris.GoO*	*-0.628*	*-1.037*	*-0.253*
E. ventermaculus.GoO	*E. guttata.GoO*	*-0.502*	*-1.125*	*0.106*
E. ventermaculus.GoO	*H. fuscopinna.GoO*	*0.750*	*0.130*	*1.344*
E. ventermaculus.GoO	*H. vulgaris.GoO*	*-1.148*	*-1.710*	*-0.584*
E. guttata.GoO	*H. fuscopinna.GoO*	*1.252*	*0.735*	*1.778*
E. guttata.GoO	*H. vulgaris.GoO*	*-0.647*	*-1.094*	*-0.148*
H. fuscopinna.GoO	*H. vulgaris.GoO*	*-1.906*	*-2.363*	*-1.449*

Table S3 | Contrasts between levels of the explanatory variable for the model testing CT_{min} differences in cryptobenthic reef fishes. Population columns highlight the contrast estimated in the model, whereas the estimate and its confidence intervals indicate estimated differences.

Population I	Population II	Estimate	LCI	UCI
C. anomolus.AG	*E. pulcher.AG*	*0.613*	*0.173*	*1.069*
C. anomolus.AG	*E. ventermaculus.AG*	*-0.400*	*-0.851*	*0.054*
C. anomolus.AG	*E. pulcher.GoO*	*0.747*	*0.316*	*1.211*
C. anomolus.AG	*E. ventermaculus.GoO*	*-1.391*	*-1.887*	*-0.888*
C. anomolus.AG	*E. guttata.GoO*	*-0.784*	*-1.241*	*-0.317*
C. anomolus.AG	*H. fuscopinna.GoO*	*-1.235*	*-1.736*	*-0.754*
C. anomolus.AG	*H. vulgaris.GoO*	*-0.080*	*-0.549*	*0.384*
E. pulcher.AG	*E. ventermaculus.AG*	*-1.011*	*-1.313*	*-0.709*
E. pulcher.AG	*E. pulcher.GoO*	*0.137*	*-0.165*	*0.446*
E. pulcher.AG	*E. ventermaculus.GoO*	*-2.003*	*-2.402*	*-1.641*
E. pulcher.AG	*E. guttata.GoO*	*-1.394*	*-1.704*	*-1.076*
E. pulcher.AG	*H. fuscopinna.GoO*	*-1.847*	*-2.206*	*-1.489*
E. pulcher.AG	*H. vulgaris.GoO*	*-0.694*	*-1.010*	*-0.358*
E. ventermaculus.AG	*E. pulcher.GoO*	*1.149*	*0.847*	*1.459*
E. ventermaculus.AG	*E. ventermaculus.GoO*	*-0.990*	*-1.382*	*-0.610*
E. ventermaculus.AG	*E. guttata.GoO*	*-0.381*	*-0.706*	*-0.065*
E. ventermaculus.AG	*H. fuscopinna.GoO*	*-0.836*	*-1.201*	*-0.475*
E. ventermaculus.AG	*H. vulgaris.GoO*	*0.318*	*-0.016*	*0.648*
E. pulcher.GoO	*E. ventermaculus.GoO*	*-2.138*	*-2.526*	*-1.766*
E. pulcher.GoO	*E. guttata.GoO*	*-1.530*	*-1.843*	*-1.213*
E. pulcher.GoO	*H. fuscopinna.GoO*	*-1.985*	*-2.341*	*-1.615*
E. pulcher.GoO	*H. vulgaris.GoO*	*-0.832*	*-1.174*	*-0.519*
E. ventermaculus.GoO	*E. guttata.GoO*	*0.607*	*0.231*	*1.018*
E. ventermaculus.GoO	*H. fuscopinna.GoO*	*0.152*	*-0.260*	*0.582*
E. ventermaculus.GoO	*H. vulgaris.GoO*	*1.307*	*0.895*	*1.691*
E. guttata.GoO	*H. fuscopinna.GoO*	*-0.453*	*-0.822*	*-0.088*
E. guttata.GoO	*H. vulgaris.GoO*	*0.700*	*0.360*	*1.041*
H. fuscopinna.GoO	*H. vulgaris.GoO*	*1.153*	*0.799*	*1.543*

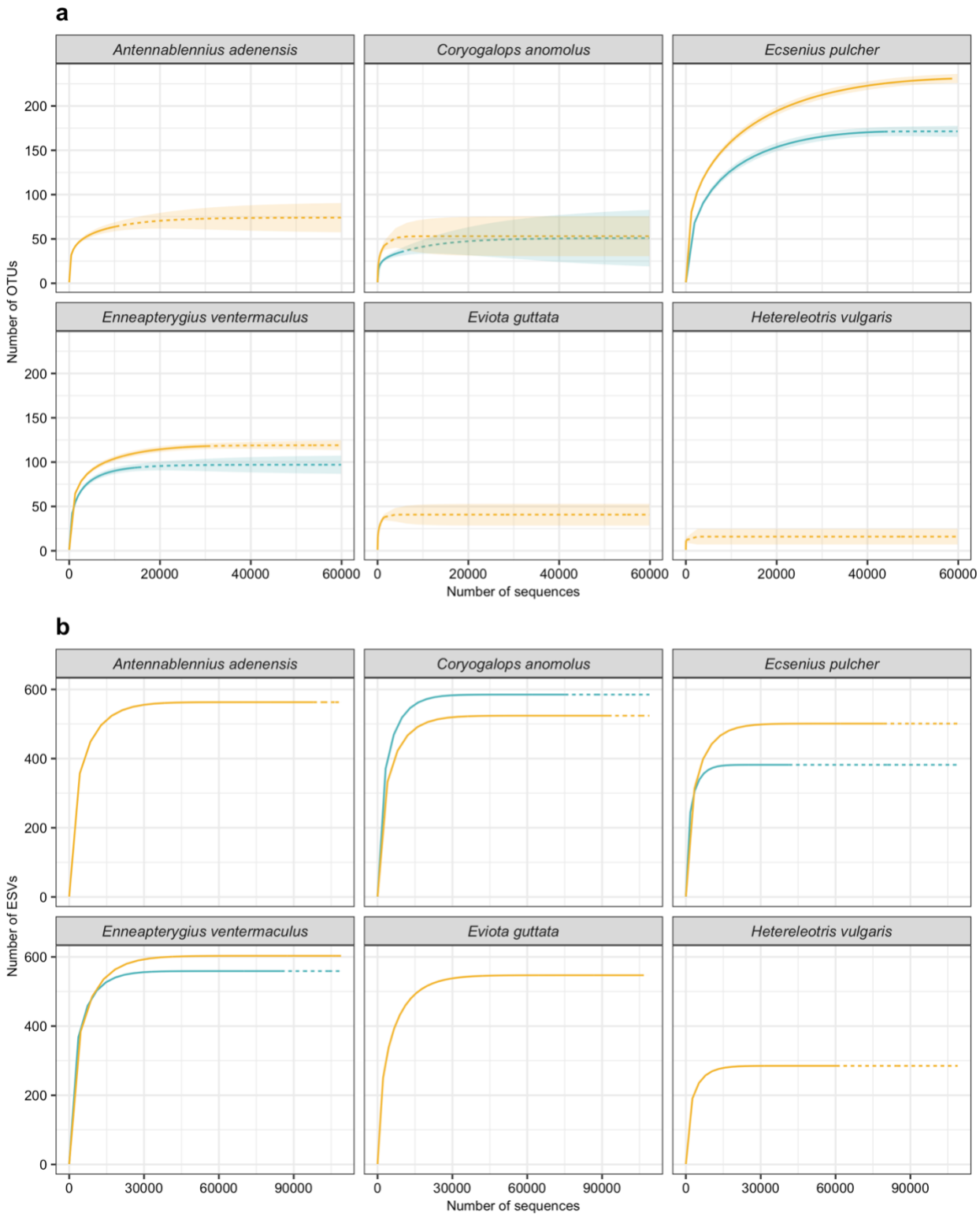

1121

1122 **Figure S1 | Rarefaction curves of OTU and ESV richness across total sequences**
1123 **for six species in the Arabian Gulf (blue) and Gulf of Oman (gold).** OTU curves (a)
1124 indicate the diversity of prey items for each species and population as obtained from gut

content DNA metabarcoding with the COI marker, while ESV curves (b) show the diversity of prey items obtained with the 23S marker. Solid lines indicate interpolated richness, while dashed lines indicate extrapolated richness (to the maximum number of sequences across species). Shaded ribbons indicate 95% confidence intervals of extrapolations.